DYNAMIC MONITORING AND DISPLACEMENT VENTILATION TO PREVENT PATHOGEN SPREAD DURING MEAT PROCESSING

A Thesis

by

ALEXANDER ALFONSO ZUNIGA

Submitted to the Office of Graduate and Professional Studies of
Texas A&M University
in partial fulfillment of the requirements for the degree of

MASTER OF SCIENCE

Chair of Committee,	Maria King
Committee Members,	Ronald Lacey
	Rosana Moreira
	Alejandro Castillo
Head of Department,	Stephen Searcy

December 2019

Major Subject: Biological & Agricultural Engineering

ABSTRACT

Shiga toxin producing *E. coli* (STEC) and *Salmonella* are two prominent bacteria that are recognized in pathogenic spread in the meat industry. In recent years outbreaks have occurred due to the ingestion of contaminated products in which could be introduced in multiple ways. A major route that has not been focused on in research and literature in the aerosolization of bacteria and the influence of airflow on bioaerosol concentration/contamination. In this study, a new method is explored in order to contribute to regulations and find an efficient solution to reduce pathogenic spread during the harvest/postharvest process in meat packing facilities. Dynamic monitoring devices, the Wetted Walled Cyclones (WWC), developed in the Aerosol Technology Laboratory, were used to acquire a representative analysis of a typical operating meat packing environment. Combined with displacement ventilation in tactical entryways throughout the facility heavy pathogenic spreading zones were analyzed and reduced. Computation fluid dynamics (CFD) was performed to assess the overall flow trajectory and visualize and validate the influence airflow trajectory has on bioaerosol concentration.

The objectives achieved through this study were to assess environmental and working conditions of a large-scale meat packing facility relative to biological growing conditions, identify facility designs specifically heating, ventilation and air conditioning (HVAC) and explore proper aerosol mitigation procedures emplacing the most efficient solution and comparing bacterial counts before and after installation. This project took place in a 13,500 sq. ft fully operational meat packing facility over a period of three years. There is little knowledge in literature focusing on airborne pathogenic spread in meat packing facilities and its contribution to pathogenic outbreaks.

The use of highly efficient monitoring devices in pairing with CFD analysis enabled testing efficient solutions for food safety and creating mitigation solution by thorough analysis.

DEDICATION

To my family: Karla, Mario, Mario, & Anis

And all my friends who got me here

ACKNOWLEDGEMENTS

I would like to express my deepest appreciation for my advisor, Dr. Maria King, for her inspiration of perseverance, knowledge, and kindness. Without her I would not be the engineer I am today, through her I truly understood the meaning dedication. I would also like to thank Hyoungmooh (Joseph) Pak, Tsz-Yi Yang, and other graduates for their assistance. Lastly, I would like to express extreme love and gratitude towards my family - Karla, Mario, Mario, Anis, and Nicole - for their encouragement and support, as I could have not done this alone.

CONTRIBUTORS AND FUNDING SOURCES

Contributors

This work was supervised by a thesis committee consisting of Advisor Chair Assistant Professor Dr. Maria King, and Dr. Ronald Lacey Professor of the Biological & Agricultural Engineering, Dr. Rosana Moreira Professor of the Biological & Agricultural Engineering, and Dr. Alejandro Castillo Associate Professor of the Department of Animal Science. Tsz-Yi Yang helped in the modification of installing the air curtain in the chamber replica. Hyoungmook (Joseph) Pak aided in the processing of the Illumina sequencing data. Dr. King aided in the collection and qPCR analysis of bioaerosols at Facility A discussed in Chapter 3. All other work conducted for the thesis was completed by the student independently.

Funding Sources

This work was made possible in part by the North American Meat Institute (NAMI).

Its contents are solely the responsibility of the authors and do not necessarily represent the official views of NAMI.

TABLE OF CONTENTS

Page

LIST OF FIGURES

Page

Page

LIST OF TABLES

Page

CHAPTER I

INTRODUCTION

In the United States economy, cattle production accounted for $78.2 billion in cash receipts during 2015. According to the USDA it accounts for the top agricultural commodities in the US representing 21 percent of the total cash receipt in a given year in the past decade. Modern beef production is seen as a highly specialized system, though it has stemmed one major problem that has been in focus for the last three decades, namely, foodborne diseases that cause outbreaks. Foodborne outbreaks are the "occurrence of two or more similar illnesses resulting from the ingestion of a common food," a definition given by the Centers for Disease Control and Prevention (CDC, (1)). These illnesses can range from mild affliction to severe life-threatening symptoms depending on the type of – bacterial, viral, parasitical, chemicals, metals and prions – etiology contaminating the food product. From this wide spectrum of contaminants, the most common bacteria patrolled for in meat packing facilities due to their severity of illness are *Salmonella* and *Escherichia coli (E. coli*) producing Shiga toxins (STEC). *Escherichia coli* symptoms are bloody diarrhea, abdominal pain and vomiting, and hemolytic uremic syndrome; attributing to the most hospitalizations in adults for foodborne illnesses (2). While *Salmonella* symptoms are essentially the same as *E. coli*, which can lead to dehydration and if untreated, death. These pathogens have a unique ability to survive in the most extreme environments or stay dormant until conditions are met for these microorganisms to reactivate and multiply.

The beef industry as a whole, starting at the farm to the fork of the consumer, provides a great example as to how these pathogens can survive, be introduced, or environmentally affected. From cradle to grave food contamination can occur or be introduced in several different ways. The source of these microorganisms can come from a healthy animal's gastrointestinal tract which during a slaughtering process can be exposed and contaminate other carcasses. Many studies have concluded that traces of pathogens can be found in the fecal matter of cattle. These pathogens are then on the cattle during the holding period right before slaughter and can survive on the cattle's hide. Thus, when cattle are brought in the meat packing facility and the dehiding process begins, these pathogens can spread traveling by different transportation routes. From these routes, pathogens can travel through cross-contamination of product, worker movement, or environmental sources (3). Environmental sources can range from high pressure washing, splashing from biofilms, and bacteria becoming aerosolized. Once bacteria are aerosolized they spread via air currents made from a facilities' heating, ventilation, and air condition (HVAC) system. Environmental conditions are taken into consideration to understand the effects they have on a facility's HVAC system. Summer months where HVAC system is running at higher speed allow pathogenic spread to occur easier. The increase of temperature and relative humidity create a better environment for bacteria like *E. coli* and *Salmonella* to thrive (4). Temperature and relative humidity play a direct relationship with one another in psychrometrics which emphasizes how the airflow of meat packing facilities needs to be further understood.

Standard detection in large meat packing facilities methods for *Salmonella* and *E. coli* are through polymerase chain reaction (PCR), multiplex PCR, and real-time PCR (5). These require culture samples in which many bacteria and viruses die off due to the insensibility of collection. Culture samples only account for cross-contamination situations, in which bioaerosols are not being taken into consideration. In the last decade foodborne illnesses caused 1800 deaths, 325,000 hospitalizations, and 76 million illnesses nationwide. Though the detection of these pathogens has been improved, foodborne illnesses still remain a prevalent problem as numbers of outbreaks are not decreasing (6). Thus a gap must be filled with current detection capabilities in conjunction with practical removal processes. Though there have been decades of research and steps toward sanitizing meat packing facilities, these steps have focused more on direct contamination processes/removal techniques. There has been less of an emphasis on research that reduces foodborne illnesses from indirect contamination sources. Very little implication, literature, and review are available on the bioaerosol movement and its role in pathogenic spread. Airborne counts found in older literature do not represent accurate measurements due to the limited equipment capability (2). Using dynamic air sampling with Texas A&M's WWC, this device enables bioaerosol collection at a flow rate of 100 L/min and a continuous liquid outflow rate of 0.1 mL/min. This allows the concentration factor of the WWC to be 0.87×10^6 for 1.2 – 8.3 μm particles with a pressure differential for the device of 6.4 inches water. The WWC aerosol-to hydrosol efficiency has a cut point of 1.2 μm aerodynamic diameter (7). This flowrate allows the collection of air to be representative

of the area of collection, while keeping the bacteria culturable in vitro compared to other collection processes.

Pairing with computational fluid dynamics (CFD) to mimic the airflow patterns throughout the facility and a profile of the bio-aerosol particle detection and warning zones can be detected. These warning zone spots will then be mitigated by different displacement ventilation techniques to reduce the amount of pathogenic concentration in that specific area. The area where these HVAC devices will be placed are the entryways before the clean zones of the facility, the chiller, the chillers, and the production room. The aim is to introduce a barrier or change in air vector direction to blow away or create a wall so the bioaerosol spread is stopped before reaching the clean sites. Thus, exploring and implementing different risk mitigation techniques will reduce and lower the potential outbreaks of foodborne illnesses.

The overall goal of this project is to contribute to regulations and find an efficient solution to reduce pathogenic spread during the harvest/postharvest process in meat packing facilities. Using dynamic monitoring bioaerosol devices, i.e. the Wetted Walled Cyclones, a representative air analysis of a typical operating meat packing environment will be acquired. In pairing with displacement ventilation in tactical entryways throughout the facility, heavy pathogenic spreading zones can be reduced. Computation fluid dynamics (CFD) will be performed to assess the overall flow trajectory of the facility and to view the changes that occur upon installation of different displacement ventilation solutions. The objectives that will be achieved throughout this study are to (1) assess environmental and working conditions of a large-scale meat packing

facility relative to biological growing conditions, (2) identify facility designs specifically heating, ventilation and air conditioning (HVAC) and (3) explore proper aerosol mitigation procedures emplacing the most efficient solution and comparing airborne bacterial concentrations before and after installation. This project took place at a fully operational meat packing facility over the span of three years. The importance of the project was to explore cutting-edge features that are now being observed in regards of food safety. There is little knowledge in literature focusing on airborne pathogenic spread in meat packing facilities and its contribution to pathogenic outbreaks. The use of our highly efficient monitoring devices in pairing with CFD analysis puts this project at the forefront in testing efficient solutions for food safety with a thorough analysis of those designs.

CHAPTER II

REVIEW OF LITERATURE

Aerosol dynamics

Aerosols are the suspension of solid or liquid particles in a gaseous medium, formed by the conversion of gases to particles and/or the disintegration of solids or liquids into finer particles. Examples of aerosols include: clouds, fog, fumes, suspended particulate matter, and smog. As the science of aerosols has developed throughout the years studies have shown that aerosols contribute to a lot of environmental factors, atmospheric chemistry, and even illnesses. The contribution to aerosols characteristics like movement, shape, mass, and concentration have abled scientist to track and describe their behavior in different settings. The main transport of aerosols are the phenomenon acting on the suspended gas. Navier-Stokes governs most equations when solving the behavior of aerosols:

$$\rho_g \left[\frac{\partial u}{\partial t} + u * \nabla u\right] = -\nabla \mathrm{p} + \eta \nabla^2 u \qquad [1]$$

where: u = local flow velocity vector, ρ_g = gas density, p = pressure, and η = dynamic viscosity of the gas. Navier-Stokes is nondimensionalized by using various reference quantities. One of the dimensionless numbers that come out of this is Reynolds number (Re) seen as:

$$Re = \frac{\rho_g UL}{\eta} = \frac{UL}{\mu} \quad [2]$$

Where: U = characteristic velocity of gas representing the whole system, and μ = kinematic viscosity.

The Reynolds number describes whether the flow is either laminar or turbulent. Laminar flow is described as when friction flow dominates the flow and Reynolds number is low around 2000 in value. Turbulent flow is considered when the flow's inertial forces dominate the streamline in which it circles back and becomes chaotic. It is more difficult to manipulate these streamlines as it disrupts proper distribution of flow. These two descriptions of flow help to understand and visualizing flow thus enabling an analysis of how aerosols will migrate in an environment (8, 9).

One environment that is important to look into is indoor settings, as the World Health Organization has reported that 90% of people spend their time indoors. Indoor aerosols originate from both indoor and outdoor sources. Indoor aerosols that come from outdoor sources originate by infiltration/penetration into the buildings through processes like air exchange, HVAC, and design of the facility. Indoor aerosols that originate indoors are linked to human activity, this includes human mechanical activates indoors in which increase particle concentration by re-suspension. Most indoor aerosols range from diameter sizes 0.1-10 μm with six orders of magnitude in particle mass (10). Size and mass are major determinants for indoor airborne particle behavior when studying deposition mechanisms like gravitational settling and inertial impaction. The focus of this study will be on the coarse particle range, 2.5-10 μm (PM2.5-10), which has been associated with

the ability to host bacterial species (10, 11). These biological species are able to attach onto surfaces from the transport movement of their host aerosol. These bioaerosols are prevalent and dangerous in facilities with human health and handling any agriculture/raw products. As smaller particles coagulate governed by Brownian Diffusion, specifically for bioaerosols this increases concentration and allows contamination. In this study, we will classify the bioaerosols studied with an aerodynamically equivalent diameter and volume equivalent diameter, meaning that the diameter standard to a sphere having the same terminal velocity when settling will classify the aerosols. Moreover, the diameter of a spherical particle will have the same volume as the particles studied (8, 9, 12).

Foodborne Illnesses in Food Industry

With the population spike brought by the 21st century, domestic food safety issues have increased in both practices inside the home and during production processes (13). In the past decade, studies have been conducted throughout the years to detect and track what the most common causes of foodborne illnesses are and what can be done commercially to prevent these outbreaks in the industry. In a ten year (1998-2008) study, it was found that land animals contributed to 42% of single etiologic agent outbreaks and an estimated 26,000 annual hospitalizations and 43% of deaths each year were contributed by land animal commodities. Though a problem with many studies and numbers tied in with outbreaks even when acquired by the CDC miss counts of unreported, not recorded by a hospital, or misdiagnosed data sets. Microorganisms are prevalent in manure and hides in meat packing facilities. The microbes living in stock pins, feedlots and pastures carry with

livestock when transported. In meat packing facilities these microbes are carried into the facility.

The most prevalent bacteria are *Escherichia coli* and *Salmonella* which causes hemorrhagic colitis, hemolytic uremic, salmonellosis, and acute gastroenteritis. These diseases known as zoonoses can be transmitted through ingestion of contaminated food, aerogenic route, or fecal-oral contact (14). *Escherichia coli,* the most commonly found in raw products affecting human health is *E. coli* O157:H7 which was first recognized in 1982 due to the consumption of undercooked hamburgers. It has been linked to other raw products like lettuce, person-to-person contact, untreated water, and raw milk. The most common serotypes of *Salmonella* are S. Enteritidis, S. Typhimurium, and S. Heidelberg. These attribute to nontyphoidal salmonellosis which is the most commonly reported infection. In the past two decades due to the modernization of the food industries centralized production and large - scale distribution incidences have doubled. Transmission of *Salmonella* has been linked to environmental sources like rodents and manure (15). The two main bacteria that will be focused on in this experiment will be *Escherichia coli* and *Salmonella,* due to their severity and prevalence in the facility used for testing.

The issue as with most bacteria is their ability to quickly adapt to their environment, become resistant against drugs, and remain dormant until proper conditions for growth. A major route in reducing bacteria in the food industry is to use antimicrobial agents. Though it has been seen in recent years that selective pressures from antibacterial agents create resistant genes in a species. These antimicrobial resistant bacteria can bypass

drugs and be passed on by conjugation, transformation, or transduction from resistant strains to susceptible strains of bacteria (16).

Bioaerosols in Meat Packing Facilities

In recent studies, the spread of foodborne bacteria is being linked to biofilms being aerosolized into bioaerosols and then traveling in air streamlines as a means of transportation. Meat packing facilities provide an enriched environment for biofilms to occur due to the moisture, liquid runoff, and multiple bacteria in close proximity with one another. Biofilms increase the survival of foodborne bacteria due to an increase of bacterial responses activating their defense mechanisms in a concentrated area. These colonies of bacteria can communicate with each other by interconnected teleonomic values in which activates response corresponding to the environment on how to adapt and survive during unfavorable conditions. (17). These interconnected signals are given off during traditional practices in meat packing facilities like refrigeration, acidity, salinity, and disinfection. These signals then turn on and off different gene expressions that will adapt the bacteria to help its survival. Paired with the increase of bacteria number, the chances of spread and survival are higher (18), allowing the development of more microbial resistance in meat packing facilities especially with a heterogeneous mixture of species within the biofilms. As the bacteria gather, they assist one another in formation, to which the structure and resistance within a community will withstand typical antimicrobial treatments (19, 20).

Naturally microorganisms occur at air-water interfaces suspension, in which they congregate to form flocs or granules. These flocs and granules associate

usually with extracellular products at interface and are typically attached either an abiotic or biotic surface (17). In combination with a facilities' HVAC system and splashback from regular production procedures, these biofilms become aerosolized. Once aerosolized, the bioaerosols can travel more freely in distance within the facility. This displays why bioaerosols are found to be the leading causes of cross-contamination through indirect contact created by air. This leads to an importance on controlling factors that help decrease biofilms and its means of transportation via aerosolizatoin. As environmental conditions change constantly through the production line it is harder to control these conditions in any standard facility as a solution. This makes the focus switch to what other design aspects can be manipulated to decrease foodborne outbreaks. HVAC design and safety should be monitored and studied to eliminate sources of potential leading issues and increased resistance with bacteria (18). In this study, one of the leading issues was that Facility A detected more foodborne pathogens once an attachment to the facility was added in order to increase production. The expansion of people, equipment, and animals increased the airborne materials and activity of that area, including bioaerosols. Stated throughout literature a standardized collection method and analytical techniques to capture and collect bioaerosols are in much of need (21).

Bioaerosol removal techniques

Dielectric Barrier Discharge

Nonthermal plasma-based technology has been used to inactivate microorganisms of both Gram-negative and Gram-positive bacteria on surfaces and in aqueous solutions. Dielectric barrier discharge brings ionized gas to an energetic state known as the "fourth

state of matter" where plasma is created. When energy increases the molecules of the gas dissociate to form a gas of atoms, these excited species act as an electrical conductor due to the presence of its free electrons and positive ions. The mechanism of the dielectric barrier discharge is based on the UVC and VUV irradiation in the wavelength range resulting in the inactivation of microorganisms due to the dissociation of their DNA strands. The high state of oxygen species causes damage by oxidation of the cytoplasmic membrane, proteins, and DNA strands in bacteria. Lastly, charged particles from the dielectric barrier discharge affect the cell wall by breaking chemical bonds and openings in the membrane in which plasma toxic enters the cell. These effects have been seen to greatly reduce microorganisms. In open-air studies it has been shown that *E. coli* had been reduced 99%, while *Salmonella* on raw poultry was reduced to 1.42, 1.87, and 3.11 log on inoculum levels of 10^2, 10^3, and 10^4 CFU respectively. Dielectric Barrier Discharge major drawback is that most application methods require flat surfaces in which meat cuts of raw products change in density, shape, and size and not possible in a major producing meat packing facility. As well the charged particles and neutral reactive oxygen can neutralize lipids thus decreasing shelf life with the quality of the product. *(22, 23)*

HEPA Filters

HEPA filters are common in most air purifiers, hospitals, and facilities in which clean air is needed for health regulations. HEPA filters use mechanical devices to trap airborne pollutants and particles within an area. By definition, they are dry-type filters with a minimum particle removal efficiency of 99.7% for 0.3-µm particles, maximum resistance when clean of 1.0 in.wg when operated of 1,000 cfm, and a rigid casing that

extends to support the filter. These filters are made out of filter mediums and separator material of accordance with provisions of ASME AG-1, FC-3000 or FK-3000. The material of the meshing is interwoven so particles higher than 0.3-µm cannot pass. Though if not clean these filters can serve as hosts for bioaerosols since microorganisms can still be active on these filters. In practical implications these filters are not regularly cleaned enough in high producing pollutant exposure environments. These filters can only remove particles that are actively suspended in the active in the air stream. Most HVAC systems have HEPA filters preinstalled, though this is not enough to stop the accumulation of bioaerosols. Other mechanisms can be paired with HEPA filters like photocatalytic oxidation. The implication of adding these mechanisms to an HVAC system can be costly and or impractical (24).

Carbon nanotube filters

Another innovative technique in bioaerosol removal is using carbon nanotube filters. Carbon nanotube filters (CNT) have been known to absorb inorganic contaminants and toxic metals in water as well as the removal of hydrocarbons, viruses, and bacteria in petroleum waster. CNT filters are made up of hundreds of individual tubes adhered by van der Waals attraction thus creating agitated mesopores. These micropores provide large surface areas in which bioaerosols can get trapped in, but small enough to immobilize biological contaminants like bacteria. Depending on the CNT different methods of purification can be applied to the allow absorption occur and remove contaminants stuck in the pores. Different treatments include: acid treatments that remove carboxyl and hydroxyl groups, increasing KOH ratios, and air activation. The absorption process of

bacteria happens almost instantaneously with high sorption and kinetic rates. The filters are placed in tubes and or filter frames in order to obtain max coverage of surface area. This medium does have issues of selective absorption in which depends on the size of bacteria. Production costs of making CNTS is impractical in large scale operations as filters can be up to $80/kg. Machines are then required for the catalyst processes to occur. The technology and capability to mass produce these filters are not feasible for large scale facilities like meat packing plants (25-27).

HVAC system – Air Curtain

Air-conditioning systems have been shown to carry activate collected biological agents as well as the ability to in-activate. Though as easily an HVAC system can in-activate microbes located on aerosols they can easily reactivate depending on environmental conditions. Small biological agents may still grow and propagate when humidity levels support growth rate conditions (25). In meat packing facilities humidity and environmental conditions change throughout the process, ranging in temperatures from: 45 - 81˚F and relative humidity from 33 -85%. Thus poses the question of how exactly using HVAC situations can benefit large scale meat packing facilities. In the meat packing industry raw meat with various mechanical devices to properly skin, cut, and freeze the carcass. Due to the sensitivity in raw production, many bioaerosol techniques are either not functional in a fast production environment or decrease the shelf life of the product. HVAC units handle air, relative humidity, temperature, and air change per hour which contributes to the local mean of air. These attributes all factor into bioaerosol concentration in indoor facilities. Thus, giving a direct reason as to why studying HVAC

unit attribution to bioaerosol concentration is an important development to scientific research. HVAC units are able to control the airstream flow directly by creating a negative pressure in the room where contamination is not wanted (28). This prevention method would limit the flow of bioaerosols to the clean areas of the facility where meat should not be exposed to any contamination. Moreover, HVAC units are already regulated and in place in facilities thus any changes or installation should be rapid and inexpensive.

Bioaerosol Collection – Wetted Wall Cyclone

Collecting bioaerosols require an instrument that will be efficient in collecting representable data for the given area while keeping the biological species viable. Two types of Wetted Wall Cyclones have been utilized throughout bioaerosols research: a batch type where aerosol particles are collected in a liquid batch that is placed on pre-set time intervals and a continuous liquid input wetted wall cyclone where a thin film of liquid is supplied to the cyclone wall and the collected bioaerosols deposited on the wall are to be transported to an external liquid distribution system (29). Determined by power, duration of testing, material consumption, and viability the wetted wall cyclone with a continuous liquid input is the better option of the two. The wetted wall cyclone has been adapted to collect bioaerosols at a wide range of locations (7). The structure of the wetted wall cyclone function is that aerosol particles are drawn by a pump system into the inlet section forming a converging flow path into the cyclone. An air blast atomizer using a tangential collection liquid injection provides a continuous spray which is typically water with 0.1% Tween-80 surfactant thus creating 40 μm droplets.

These droplets are then carried by airflow to a rectangular cyclone inlet slot, where they will be directed by a vortex finder inside the cyclone body. The droplets will impact on the inner wall of the cylindrically shaped cyclone body where air shear will then develop the droplets into a liquid film traveling in an angular direction. After one revolution around the cyclone body, the film interacts with roughly 25-50 m/s velocity air jet effluxing from the inlet slot. The liquid is re-atomized to droplets to the cyclone wall where they will coalesce with the liquid film. The axial-component of the air shear transports the liquid away from the inlet slot to where the liquid will eventually form rivulets from droplets due to surface tension. These rivulets travel along the surface wall to the skimmer entering a gap between the nose of the skimmer and the inner diameter of the cyclone. Once in the gap, the entrapped liquid is then aspirated from the cyclone by an external pump and into a collection vial for the hydrosol.

The WWC is designed geometrically similar and based primarily on Stokes and Reynolds numbers.

$$\text{Stk} = \frac{C_a \rho_w D_a^2 U_i}{18 \mu w} \quad [3]$$

and:

$$\text{Re} = \frac{\rho U_i w}{\mu} \quad [4]$$

Here: C_a =Cunningham's correction (30); ρ_w =density of water; D_a =aerodynamic particle diameter; U_i =speed of air in the inlet slot; μ = air viscosity; ρ = air density; and, w =slot width.

To this experiment the WWC is based on three performance parameters: aerosol-to-aerosol collection efficiency (η_{AA}), aerosol-to-hydrosol efficiency (η_{AH}), and concentration factor, (CF).

The aerosol-to-hydrosol efficiency describes more of the performance of the WWC as it is defined: as the ratio of the rate particles of a specified size leave the cyclone in the hydrosol state to the rate they enter in the aerosol state, it is expressed as such:

$$\eta_{AH} = \frac{c_{l,e} Ql}{c_{a,\infty} Qa} \qquad [5]$$

where: $cl,_e$ =concentration of particles of the specified size in the hydrosol state at the liquid exit port; Q_l =volumetric flow rate of liquid at the exit port; and Q_a =volumetric flow rate of air at the cyclone entrance port in short the aerosol sampling flow rate.

The concentration factor is dependent on the aerosol-to-hydrosol efficiency and is expressed as such:

$$CF = \frac{Q_a}{Q_l} \eta_{AH} \qquad [6]$$

(31). Thus, the WWC collectors will be used in this study due to their high efficiency rate and viability of biological presence found in samples compared to collection devices. Other collection devices for bioaerosols include single and multi-stage impactors, filters, impingers, and electrostatic precipitators though they do not have the capability of the WWC. (12, 32, 33)

Computational Fluid Dynamics in Indoor Air Modeling

Computational fluid dynamics is a new approach and recently widely used to

explore bioaerosol transport in facilities, hospitals, and residential homes in order to acquire indoor air analysis profiles (34-36). CFD uses algorithms and equations from natural and dynamic phenomenon to predict the physics of flow within the desired area programmed (37). Discretion schemes are used within the model in order to represent the continuous equations used for the system. Meshes are made within the model creating a 3D vector grid where each mesh takes into account the schemes used and displays and shows how each vector acts within that mesh (37, 38). The finer the mesh the higher the accuracy of the model becomes as movement of flow is broken down into smaller vectors. These meshes represent the faces where boundary conditions and goals are specified. A more finer mesh has more cell numbers which create a more accurate geometry to increase the performance of the model (38). These schemes can be best fit by describing the environmental and mechanical influences of the system. Once these sources are determined numerically through experimental studies, governed equations are changed to match similar to layout and airflow mechanics. These studies are held by restraints of environmental conditions such as worker movement, machine equipment, and product transport (39).

Indoor CFD mostly uses scales and the concept of mass-balance-conservation within a basic model to track movement. Most indoor aerosol models incorporate deposition, resuspension processes as well as emissions from indoor activity sources. There are two major types of models when creating CFD airflow models: the single compartment and multiple-compartments. In this case, this environment would hold to a

multi-compartment model since there is more than one contaminant of aerosol occurring in the space. Multi-compartment models tend to have difficulty with accuracy due to dependencies like mixing, consequences of indoor activities and spatial gradients (40). Due to the focus of the study, Facility A will be treated as a single-component model which would give the characteristics of only one dynamic behavior of only one pollutant. Since this study is focused on bioaerosol interaction the different organisms will be grouped as one. Outdoor exchange rates will not be taken into account due to the mass size of the facility and environmental changes in conditions during each process in the meat packing facilities. Since we do not know the aerosol profile outside of Facility A we cannot estimate the number of particles infiltrating the HVAC system.

In acquiring an accurate CFD model to replicate experimental results and the overall project environments different environmental aspects play into the dynamics of the model. In indoor air quality models air temperature stratification and the local mean age of air are developed by solving a system of equations. In most indoor air quality models the standard k-ε model is used which solves a system of equations made up by Reynolds-Averaged Navier-Stokes. solved in (35). A standard k-ε model describes the kinetic energy of turbulence and its rate of dissipation, ε (34). Gilani et al noted that temperature influences the standard k-ε models while an iterative convergence criterion affects the local mean age of air in a model.

Once solved the solution then shows the behavior of the airflow with environmental factors taken into consideration. In combination with the combined boundary conditions from the intakes and exhausts the airflow of a facility is then created. This design data can

then be used in order to create a standard for ventilation construction in order to manipulate the airflow however desired. There is very little literature on using CFD and bioaerosol analysis to track, predict, and mitigate contamination. This route of investigation allows a more economical process of implementation and creates a template for other meat packing facilities. These templates would help the food processing industry not only in modern production, but in providing insight for a growing population and developing countries when building these facilities. Given the public attention of outbreaks further investigation can help the sustain shelf life of products (41).

Analysis of Bioaerosols

As new methods of analyzing microbes have been discovered the standards for acquiring bioaerosols have not been set in indoor environments. Before the process of analyzing the bacterium found during collection, understanding the analysis method for post-processing needs to be understood. In this study, two methods of bioaerosol analysis will be used, namely culture based and quantitative PCR. In study and standard most indoor bioaerosol data is collected and monitored through culture based analysis. Culture based analysis involves the examination of bioaerosols through agar plates, one of the oldest methods used in practice. The process of agar plating allows the bacterium to be incubated on the medium and inspected for colony forming units (CFU) and total viability count (TVC). The counts can be divided by the total volume of air sampled to determine the number of bacteria present during collection. Though in this manner collection is limited in accuracy due to the inability to account for bacteria that have been harmed during collection and cannot grow into colonies. This includes other species outcompeting

each other and bacteria not forming colonies since the agar can be selective against other species (29). In this study part of the microbial analysis was done using the culture based analysis used described above, with direct spreading onto a casein soy peptone, and tryptic soy agar. These two media are simple media which have the nutrients and ability to support the growth of most bacterium. This collection method allows a snapshot of the microbial contamination and concentration in the area. The quantitative process of real PCR was used in the genome analysis and allows genotypic identification of the bacterium found. This type of identification doesn't need the bacteria to be viable as long as the DNA of the bacteria is intact, allowing different means of capture for the bioaerosols devices. In the PCR process, the DNA is amplified exponentially where they can be analyzed, a method that is not as selective or extensive in incubation time.

Lastly to conclude the most advanced technique of bioaerosol analysis used in this study was genomic sequencing techniques. A single amplicon can describe the entire microbiome and map every percentage of bacterium found in the sampling medium, not just only the concentration. The genetic sequencing technique used was Illumina DNA sequencing which utilizes broken down DNA fragments, from 200 to 600 base pairs. These pairs undergo four major steps: library preparation, cluster generation, sequencing, and data analysis. During library preparation the DNA fragment samples sequences by 5' and 3' adapter ligation into a sequencing library randomly. This preparation method is the combination of fragmentation and ligation into a single step. Once completed the adapter-fragments are PCR amplified and gel purified. The next step is cluster generation, where the library is loaded into a flow cell where fragments are attached to surface-bound oligos

complementary to the library adapters, any DNA that is paired displays a signal which is picked up by a camera. Each fragment is then amplified (by nucleotide bases and DNA polymerase) into precise clonal clusters ready for sequencing. The Illumina Sequence processor uses a proprietary reversible terminator based method where fluorescent terminators that correspond to the different bases – (A, C, T, G) – are present during the sequence style at the same time. Thus, when a laser passes over, it is then detected by a camera and recorded. Lastly, the DNA is then read and aligns to a reference genome (42). After this sequencing process an analysis tool, in this instance, Quantitative Insights Into Microbial Ecology (QIIME 2) was used to evaluate the percentages and relations occurring in the microbiome of the sample and create ready images of the microbiome data.

CHAPTER III

METHODOLOGY

Overview

Air samples were taken collected in a full-scale 13,500ft^2 meat packing facility (Facility A) over the span of two different instances during the Spring/Summer seasons. Facility A practices the typical processes – stunning, bleeding, skinning, evisceration, splitting, washing, chilling, rendering, and packaging – that most typical meat packing facilities go through to obtain revenue. In such a large facility, a major concern is to find a device that is efficient, heavy-duty, and discreet in order to collect quality air samples. Due to the large size of the facility multiple devices with efficient air collection rates are needed to assess the air quality for the area it will be placed in. Mobility is required for the devices in order to make a comparative analysis with respect to time for a representative overall sample. As Facility A is industrial, the devices cannot stop business production or disturb any process in an average work day. Using a patented product of A&M and the US Homeland Security, we used our bio-aerosol Wetted Wall Cyclone as it fits each characteristic described above and able to collect a representative environmental sample. The bioaerosol Wetted Wall Cyclones were used at 100 L/min, sampling at four hour shifts, broken up between morning and afternoon worker shifts. Falcon tubes collecting the hydrosol were changed out if sample volumes were too large during testing time. The sampling locations in the facility were focused on the major dirty areas and the specified clean areas in a large scale meat processing facility. Once the total samples for

that day were collected, processed, and analyzed by spread plating and quantitative polymerase chain reaction (qPCR) the TBC of the facility at every location was determined. STEC *eae, stx,* and *inv*A were also determined, as well sent in for Illumina sequencing. An airflow model using CFD was made for the specific site, paired with the dynamic monitoring technique, and an analysis to monitor heavy warning zones was conducted. Studying these zones, air mitigation techniques were explored to reduce bacterial count. An air curtain mitigation solution was then implemented to the CFD analysis of the entire facility. To validate the model an air curtain was installed into a chamber to replicate its function in a facility. Anemometers were then used to obtain velocity mappings of the flow distribution from the air curtains. To create a template for other facilities to reduce pathogenic outbreaks, our objectives were the following:

1) Assess the environmental and working conditions of a large scale meat packing facility through dynamic air collection,
2) identify facility designs and heating, ventilation, and air conditioning (HVAC) characteristics that cause pathogenic spread, and
3) explore proper aerosol mitigation procedures, emplace the most efficient solution, and determine if successful by recollecting and comparing bacterial counts.

Hypothesis

1. High velocity air units at cattle entrance create a high concentration of aerosolized bacteria, this concentration increases with higher temperature and relative humidity.

2. Complex and complicated facility design creates more turbulent air vortexes for pathogens to survive and spread into clean areas of the facility.

Placement of air curtains at the entrances of clean zones and at locations where large air vortexes are formed will reduce pathogenic spread.

Assessing Environmental and Working Conditions of a Large Scale Meat Facility through Dynamic Air Collection

The WWC uses a tangential impactor which reduces the mechanical stress on the bacteria collected in a bioaerosol sample and maintains the culturability and DNA integrity of the cells. The functions and inner workings of the WWC can be seen in Figure 1. Compared to an 800 L/min inertial impactor the culturability of *E. coli* is two magnitudes higher with the WWC in room temperature and 4000 higher in 46˚C which is commonly found in meat packing facilities (7, 43).

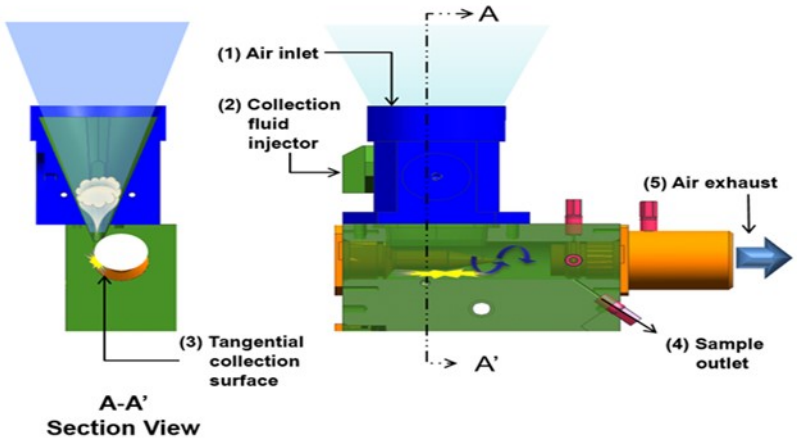

Figure 1. Diagram of the functionality of the WWC viable bioaerosol collectors. In the diagram following the numbers. (1) Collection of aerosol particles starts with particle laden air being drawn into the Air Inlet. (2) Atomized collection fluid is injected into the air stream. (3) The collection fluid and particles impact on a tangential collection surface, entraining the particles in liquid. (4) Air shear continuously transports the fluid from the collection surface toward the exhaust. The liquid sample is skimmed off the continuously extracted at the sample outlet, (5) The airflow then exits the exhaust.

In spring and summer 2017, five WWC units were placed throughout the facility to ensure that the collection times of the air samples were distributed evenly to acquire real-time samples that would equate to an average working day. This allowed comparisons to be made on the bacterial count and trends of the overall facility and between each site as the day continued. This real-time capture with dynamic sampling enables to see if there was a trend that occurred as the day progressed, comparison of rooms whether higher counts were found, or if there is a shift in the microbiome composition due to location/activity. The sites we focused on in Facility A were: Dehiding Area 1, Dehiding Area 2, Tripe Room, Chiller and Fabrication Room (Figure 2).

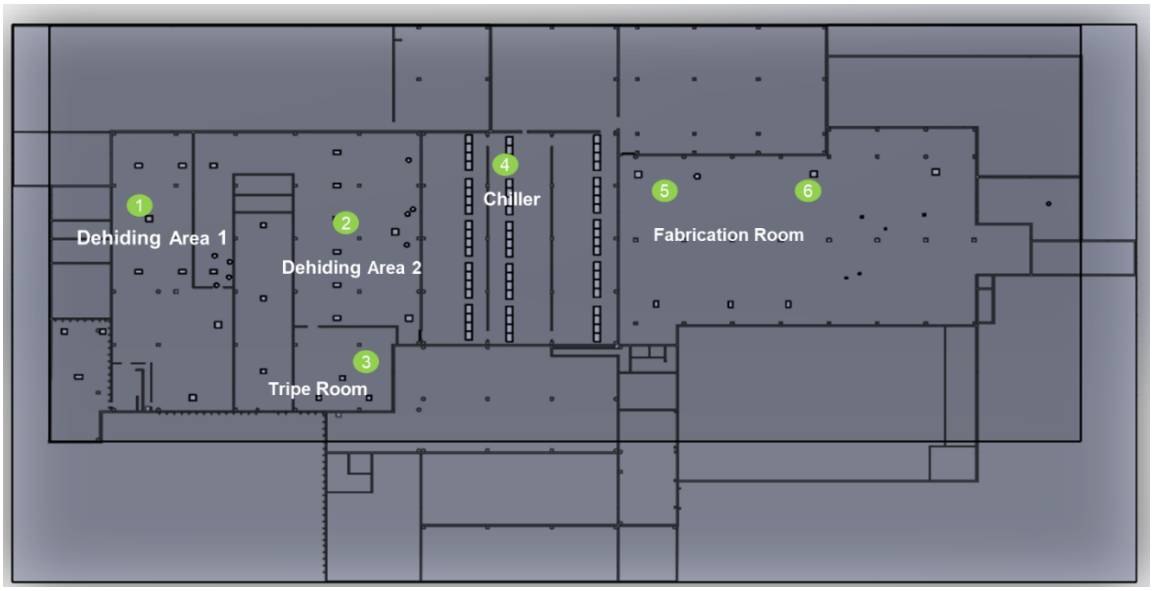

Figure 2. Top view of the CFD model of Facility A. Indicated by numbering are the five major rooms with green dots for the placement of the WWC in the facility.

The WWC collectors were thoroughly washed before collection with 10% bleach, followed by isopropanol, and finished with sterile Milli-Q water. After washing the collectors were ran for approximately 10 minutes to ensure that no residue was left in the tubes. The hydrosol was captured in a 50 mL falcon tube and after collection all samples were put on ice. The WWC was placed before the slaughtering process of the cattle begin and ran all through a working day. It is noted that an average of 1800 cattle is processed at Facility A daily. Though locations 1 and 2 have the same name of function for the room, there are differences in the processes. Location 1 is where the steers are knocked, exsanguinated, and skinned by an automatic hide puller. Location 2 is where the evisceration, splitting, and washing occur leading to either the tripe room or the chiller room to be chilled. It can be noted

that due to the high concentration of bacteria found in steers' hide, the dehiding process causes the release of most bacteria due to the machinery's pulling mechanism. Location 5 was moved to location 6 in order to capture the full area of the fabrication room. The falcon tubes of bioaerosol hydrosol samples were collected periodically, labeled and marked for the hours of duration they represent. To capture the relative humidity and temperature of the facility for a full environmental profile HOBO data loggers were placed and operated continuously next to each WWC. Since bacteria can stay alive and airborne for hours after aerosolization within the range of temperature (10-30˚C) and relative humidity (40- 80%) (44), records of these properties were taken. These environmental parameters can give hints as to the different temperatures and relative humidity changes that occur seasonally, throughout the day, and in-between the slaughtering and cleaning process. Trend graphs were made through HOBOware with the HOBO logger data to acquire a line graph of the temperature and relative humidity for each HOBO unit. The logger has an accuracy of +/- 0.95 °F and +/- 3.5% RH and was set to sample every five seconds. The main HOBO data was analyzed in the dehiding areas and the fabrication room since there is a larger variety of environmental changes occurring in these rooms.

Identify Facility Designs and Heating, Ventilation, and Air Conditioning (HVAC) Characteristics that Cause Pathogenic Spread

Creating SolidWorks Flow model of Facility A

Once the environmental profile of Facility A was acquired with bioaerosol samples obtained, a computational fluid dynamics model was created in order to understand how pathogenic spread occurred. For this project, SolidWorks Flow was used to build the

airflow model to scale virtually. Blueprints of Facility A were be obtained as a .dwg file and transformed over file to the modeling platform, SolidWorks Flow. The building is a full up-to-date replica of the running facility, the assumption is made that the doors were not to be included in the model. Since carcasses moved through a conveyor belt and people were walking in and out of different rooms continuously doors would create an illogical barrier within the facility. Doors were only to be emplaced in the office areas, however, since there is a distinct clean area zone. air movement throughout those zones were not of focus. Equipment and conveyor belt systems were not included as well, since machinery would be considered negligible to airflow pattern movement. Structurally Facility A was created in a hollow manner like a shell though columns and pillars were still included. In the primary stages, the model was be made simplistic to focus on the flow trajectory created by the HVAC units.

Creating SolidWorks Flow Analysis profile

The SolidWorks package uses a Cartesian-based mesh, which rectangular cells are adjacent towards one oriented along the Cartesian coordinates. The cells are then intersected by the surface according to the boundary condition defined by the user. The cells are then determined if they are solid cells, fluid cells, or partial cells (containing both fluid control volume and solid control volume). This is how the geometrical parameters of a volume and the coordinates of the cell center are calculated based on the model. In the flow regions to calculate transient flow the simulation solves continuity equation and Navier-Stokes as Eq. 7 and 10.

$$\frac{\partial \rho}{\partial t} + \frac{\partial (\rho u_i)}{\partial x_i} = 0 \qquad [7]$$

$$\frac{\partial (\rho u_i)}{\partial t} + \frac{\partial}{\partial x_j}\left(\rho u_i u_j\right) + \frac{\partial P}{\partial x_j} = \frac{\partial}{\partial x_j}\left(\tau_{ij} + \tau_{ij}^R\right) + S_i \qquad \text{i = 1,2,3} \qquad [8]$$

Turbulent flow of hydraulic fluid in this model is assumed on a time average quantity. Since the actual flow has unknown variables related to Reynolds' Stresses, mass fluxes, and turbulent heat these properties are given constants. In order to get proper turbulent modeling the damping functions by Lam and Bremhorst describes laminar, transitional, and turbulent flow of homogenous fluids (45). This model consists of these two turbulence conservation laws expressed by the equation of turbulent energy (k):

$$\frac{\partial (\rho k)}{\partial t}\frac{\partial (\rho k u_i)}{\partial x_i} = \frac{\partial}{\partial x_j}\left[\left(\mu + \frac{u_t}{\sigma_k}\right)\frac{\partial k}{\partial x_i}\right] + \tau_{ij}^R \frac{\partial u_i}{\partial x_j} - \rho\varepsilon + \mu_t p_B \qquad [9]$$

and the equation of turbulent dissipation rate (ε):

$$\frac{\partial (\rho \varepsilon)}{\partial t}\frac{\partial (\rho \varepsilon u_i)}{\partial x_i} = \frac{\partial}{\partial x_j}\left[\left(\mu + \frac{u_t}{\sigma_\varepsilon}\right)\frac{\partial \varepsilon}{\partial x_i}\right] + C_{\varepsilon 1}\frac{\varepsilon}{k}\left(f_1 \tau_{ij}^R \frac{\partial u_i}{\partial x_j} + C_B \mu_t p_B\right) - f_2 C_{\varepsilon 2}\frac{\rho \varepsilon^2}{k} \qquad [10]$$

Where: S_i= a mass-distributed external force per unit mass, τ_{ij}= μS_i, τ_{ij}^R= $\mu S_i \frac{-2}{3}\rho k \delta_{ij}$,

S_{ij}= $\frac{\partial u_i}{\partial x_j}$+$\frac{\partial u_j}{\partial x_i} - \frac{2}{3}\delta_{ij}\frac{\partial u_k}{\partial x_k}$, p_B= $-\frac{g_i}{\sigma_B}\frac{1}{\rho}\frac{\partial \rho}{\partial x_i}$.

When:

$C_\mu = 0.09$, $C_{\varepsilon 1}$= 1.44, $C_{\varepsilon 2}$= 1.92, σ_k= 1.0, σ_B= 0.9, σ_ε= 1.3, C_B= 1.0, if $p_B > 0$, C_B = 0,

if $p_B < 0$, the turbulent viscosity μ_t is determined by $\mu_t = f_{ij} \frac{C_\mu \rho k^2}{\varepsilon}$. Once the system of equations are solved a flow profile is made. This profile characterizes laminar flow with Reynolds Number if $Re_\delta = \frac{\rho u^e \delta}{\mu} < 4000$. u^e is the fluid flow velocity at the boundary layer's fluid boundary. Assumptions made in this model made associated with the fluid boundary would be that the walls of the facility were considered adiabatic. Heat conduction in solids were not represented in the model due a limiting factor from SolidWorks' capability. Temperature and relative humidity for the CFD model made was determined by the averages acquired in both HOBO data sets between the dehiding and fabrication room, from both spring and summer sets. Relative humidity was set to 64.51% and temperature was set at 61.91˚F. Pressure was set to static standard pressure, 2116.217 lbf/ft^2 and assigned to major openings to outdoors found in the dehiding area.

The boundary conditions, the HVAC units within the system were installed by cutting holes in the roof of Facility A relative to the size and shape of the inlet and or outlet. Lids were created for each inlet and outlet in order to create a surface boundary where each HVAC unit within meat packing Facility A be assigned. The HVAC flow rates within Facility A were assessed and reported by the Environmental Technical Services in 2015 Facility. There were a total of 18 exhausts with flow rates ranging from 3,801-22,460 cfm, while there are 4 inlets with flow rates ranging from 51,801-59,945 cfm. Once each inlet and outlet was assigned with its respective boundary condition (volumetric flow rate) an environmental profile was be created specifying gravitational, temperature, and relative humidity properties. The liquid of use to conduct the CFD was a standard composition of

air. For Facility A the cleanest area needed, the fabrication room, does not have HVAC inlets running during production, which creates a negative pressure designed room to isolate the packaged products from aerosols and contaminants. The model focused on energy and dissipation due to the large size of the facility and that the majority of focus in this study was airflow trajectory. Once the environmental and boundary conditions (inlet, outlet, and pressure) for Facility A were set the model was then considered fully defined. The total mesh consisted of 584,747 cells and twenty-two hours to complete 697 iterations. The resolution of the SolidWorks Flow is based on the resolution of the Naiver Stokes equation described above in conjunction with a two scale wall function This method divides the computational domain into elementary volumes around each node of the meshing grid, providing continuity of flow between nodes. Through a tetrahedral interpolation scheme, a spatial discretization is obtained, and for temporal discretization, implicit formula is adopted depending on the environmental parameters (38). The simulation was running for the same amount of time as a full working day in real life for Facility A, for approximately nine hours. The CFD was conducted on a fast processor computer provided in the Center for Agricultural Air Quality & Engineering Science lab. Once the simulation was complete, three different flow trajectory profiles were made highlighting the flow trajectory made by the inlet and by the outlet separately, then lastly overall. The flow trajectories gave multiple vector arrows and a velocity gradient scale showing the airflow of Facility A. Once the different flow trajectories were created an analysis was done viewing the different profiles and identifying the regions that had the most turbulence causing warning zones. These areas will be noted.as large vortexes will

recirculate dirty airflow. Thus, allowing the impaction of bioaerosols to be more prevalent due to an increase of concentration. To further investigate the air changes and how often clean air is introduced within the facility the local mean age of air was analyzed to confirm if the circulation within the units is functioning correctly.

Explore Proper Aerosol Mitigation Procedures, Implement the Most Efficient Solution, and Determine If Successful by Recollecting and Comparing Bacterial Counts

Subtask 3a: Explore and Implement Proper Aerosol Mitigation Procedures

Prior to this study research has shown that small scale displacement ventilation has been proven effective to reduce pathogenic spread. (46) It has been seen to increase sanitation low level, air stream jets can be placed within the facility at a rate of 5 ft/s. This action as well should blow laminar flow in the direction of clean air locations towards the dirty air location. In regards to this project, the facility is already built, thus installment of the HVAC system must be simplistic and economical since the facility will be in production. The goal was to create the most optimal airflow trajectory profile in which these large vortexes are not present in clean areas within the facility and create a more distinct barrier of air separating between the clean and dirty areas within the facility. An air curtain was implemented between two locations of the facility, (1) in the doorway between the dehiding area 2 and the chiller and (2) the doorway chiller and the fabrication room running at its highest speed found in industry at 5 ft/s. SolidWorks Flow modeling was implemented when the flow analysis was done. The total mesh consisted of 807,354 cells which took twenty three hours with 788 iterations. The same analysis was done over this flow profile as described earlier.

Subtask 3b: Evaluation of New Design v. Old & Overall Bacterial Quantification

The collected bioaerosol samples were plated for microbial analysis and compared to the different collection locations. To determine if the concentration of *Salmonella* and *E. coli* were detectable within the facility, method of FSIS Microbiology Laboratory Guidebook, Chapter MLG 4.08 was adapted for the air samples. This was done by plating an aliquot of the sample onto universal tryptic soy agar (TSA, Becton-Dickinson) and selective XLD agar plates, incubating overnight at 37˚C, and enumerating for CFU for qualitative analysis. DNA extraction and amplification associated with qPCR was conducted for all the bioaerosol samples to quantify and identify the samples. The samples were tested using non-enrichment, whole-cell quantitative Polymerase Chain Reaction (qPCR) method using 16s rRNA based primers and STEC/*Salmonella* specific oligonucleotide (47, 48). Once separated into DNA isolates, each sample was sent to the Texas A&M's institute for Genome Sciences and Society for Illumina sequencing. Each sample's Illumina sequence was then analyzed in QIIME to understand the microbiome of each location. This gace a greater knowledge of the overall bacterial profile and indicate which species of *E. coli* or *Salmonella* are predominant and if they are comparable with the previous studies at our department. Moreover, through QIIME a taxonomic assignment, phylogenetic reconstruction and diversity analysis was performed to provide a better characterization of pathogens in Facility A.

Plating

Direct plating was performed before and after the enrichment of each sample by spread plating a thin layer of selective media which is overlaid with non-selective media. This method increases the recovery of sub-lethal injured cells and the number of organisms. This sample was then plated onto a thin agar layer (TAL) medium. The petri dish media had a 25 mL agar added till a height of 6 mm with 14 ml of TSA overlaid in a 7 mL two-step process. The top layer with a 3-4 mm thickness, was solidified and used when ready. To enumerate *Salmonella* colonies, XLT-4 agar was overlaid with TSA media. The samples were incubated at 35˚C for 24 hours. The plates with typical colony formation were further investigated for confirmation of species. Serological and biochemical tests were carried out for colonies to identify *Salmonella.* Real-time PCR oligonucleotides were used in order to conduct the qPCR.

DNA Extraction

To extract the DNA from all the samples, an Alkaline Lysis method was used. The samples were pelleted in an Eppendorf centrifuge for five minutes at 13,000 x g. The pellet was resuspended in 300 µL TENS, vortexed at low speeds for about twenty seconds, and incubated for ten minutes at room temperature, then put on ice. Once chilled, the proteins were precipitated by adding 150 µL of 3N sodium acetate and centrifuged at 13,000 x g at 17˚C. The supernatant was then transferred to a separate 1.5 mL microcentrifuge tube. An aliquot of 10 µL of Poly Acryl Carrier (PAC, Molecular Research Center) was added to each tube with supernatant then inverted. The DNA was precipitated with 1 mL of 100%

isopropanol, inverted ten times until it was well mixed, then placed in a centrifuge for a twenty minute duration. After centrifuging the isopropanol was removed, the pellet was washed with 1 mL of ice cold 100% ethanol and vortexed until the pellet was released from the bottom of the tube. After the tubes were centrifuged for ten minutes and the supernatant was removed, the pellet was dried and dissolved in 50 µL of sterile Milli-Q water. Using NanoDrop Technology, the DNA concentration was measured based on absorbance (A_{260}/A_{280}) using a spectrophotometer.

qPCR

Different virulence gene expressions were used when performing qPCR to characterize and quantify the specified bacteria. For *E. coli*, two genes were selected: *stx* and *eae.* The gene *stx* of *E. coli* represents the Shiga toxin gene while the *eae* represents the Enteropathogenic *E. coli* (EPEC attaching effacing A gene) found in STEC. Both genes are precursors to *E. coli* and can be expressed individually in a sample area with contamination. The gene sequence to determine if *Salmonella* was present was *inv*A which is the genetic locus that allows *Salmonella* spp. to enter cultured epithelial cells. The extracted DNA (3 µL of hydrosol sample supernatant) is added to the qPCR tubes containing qPCR assay reagents and amplified in a thermocyler/analyzer. The extracted DNA is added with a master mix which contains 1 µL of Reverse and Forward primer for the specific genes described above with 5 µL of 2 X SYBR Green PCR Master Mix. SYBR Green is a fluorescent dye that indiscriminately binds to double-stranded DNA which then makes the amount of signal depending on the mass of product created (49). The AB StepOne RT-PCR System (AB, Foster City, CA) thermocycling program had an initial

cycle of 95ºC for ten minutes followed by forty cycles at 95ºC for fifteen seconds and at 60 ºC for 60 seconds. After the qPCR was completed a melting curve was created in the range of 60-90 ºC where positive amplification occurs. The samples of qPCR are then cooled to 65 ºC and then heated gradually by 0.2ºC/s to 95ºC. After the process is complete the DNA strand separation at the melting point by a large reduction in fluorescence. To confirm amplification specificity the fluorescence signals were used for continuous monitoring. The number of cells in a sample count by the threshold is defined as Ct, in which Eq. 11, by King and McFarland (2012), is used to calculate GCN/m^3 air.

$$C_{CFU} = e^{(\frac{34.1-Ct}{1.35})} \quad [11]$$

The number of cells in a sample found by real-time qPCR which will give of a Genomic Copy Number (GCN) that is proportional to the threshold value of DNA quantification, defined as Ct, which depends on the total number of DNA in a sample. The threshold value is used to relate the logarithm of bacteria concentration in a sample, with higher values of Ct associated with smaller values of concentration. The equation above is based on LIVE/DEAD BacLight™ Bacterial Viability Kit of a stock suspension each test or calibration data point showing the relationship of Ct. There is a 90% ratio of culturable cells directly to the total number of cells. DNA of samples located in positions of interest was sent to the Texas A&M sequencing laboratory.

Subtask 3c: Create replication and simulation of the air curtain solution to show its effect on the bioaerosol and air movement and validate CFD.

Due to time constraints and resources with Facility A, air curtains cannot be placed in the facility at this time to see if they will minimize key spots and stop bio-aerosol

transportation. To acquire this data a replication of an entry doorway from Facility A will be recreated in a chamber. The chamber used was originally constructed for NIH hospital studies to reduce particle concentration within a hospital room setting using various air exchange rates (50, 51). For this experiment it was configured to act as an entry found in Facility A. A separate CFD model of this chamber with the air curtain will be created in order to collect data and visualization of the new airflow direction introduced. The CFD will give insight on how the real life replication should verify with the model. With both the replication and simulation verified numbers and equations can be obtained to then implement with the larger facility to validate that model. The chamber will represent a scaled version of the entryway if it were in an isolated area. Then a 2ft width air curtain will be placed above the doorway as if it were in the actual facility. The door will be open as the entryways are all open in Facility A. Velocity profiles will be captured using anemometers attached to stands inside and outside of the chamber with the air curtain running in order to validate the CFD model. The anemometers were placed 38cm across from each other making up three rows of displacement. For each row, the anemometer was raised 41 cm for every measurement to get a total of 15 velocity points. This was done 12.7 cm away from the doorway in both directions of the doorway. This would create a velocity profile of 30 points. These measurements were captured 3 times and averaged. Once the validation of velocities is shown, the flow direction feature in SolidWorks Flow will be used to visualize how bioaerosols will flow in a large facility setting. Depending on the results it would be suggested for implementation to older facilities. Based on the

CFD models a guideline can be written on limitations and procedures that should be followed when constructing a facility.

CHAPTER IV

RESULTS AND DISCUSSION

Spring Facility A Bacterium Analysis

The first set of bioaerosols that were sampled at Facility A was from a two-day sampling period in the spring, with the first day only sampling in the afternoon and the second day both morning and afternoon. The bioaerosols collected were categorized into Total Bacteria Count (TBC), STEC *stx*, and *Salmonella* concentrations in genomic copy number related to cubic meter (m^3) of the collected air. In the first set, the only STEC was tested using the primer *stx* for qPCR. The samples collected were further characterized by their time of collection, which day the sample was taken, and the location within the facility. Quantitative PCR was performed to enumerate the total bacteria count. The three data sets of GCN/m^3 air samples collected were calculated and plotted (Figure 3). For TBC the least bacteria were collected in the morning with levels lower than 1000 GCN/m^3 air and the most bacteria were collected in the dehiding room and tripe room, approximately 4,500 GCN/m^3 and 5,800 GCN/m^3 respectively. A positive correlation ($P>0.5$) can be found between the bacteria counts and as the day progresses throughout the day. This can be due to an inefficient HVAC design in which the circulation could lead to accumulation of bacteria throughout the day. At Facility A 1,800 heads of cow per day is processed with two breaks in the morning and afternoon. As they are broken up throughout the day the facility is hosed down in the dehiding locations 1 and 2. The spraying of the facility floor

could introduce aerosolization of such bacteria, in addition to the introduction of more bacteria when each new head of cow is introduced.

STEC *stx* samples were only significantly found in the morning in the dehiding area with approximately 125 GCN/m^3 showing no sign of significant decrease compared from Day 1 to Day 2. There was no significant correlation ($P<0.5$) found between the two days. With the aerosolized *Salmonella* there was no significant difference between both days or in the morning and afternoon. There was no collection on the first day of the afternoon nor the morning of the second day. Counts were found in the dehiding area and tripe room of the facility where it was to be expected as these two rooms are both dirty areas of the facility. The counts were 43 GCN/m^3 and 38 GCN/m^3 respectively. In regards to TBC it can be inferred that the significant increase in bacteria related as the day progresses can be due to multiple factors such as the increase of workers, continuous introduction of cow head, and/or poor design of nonsingular movement HVAC system. This would allow aerosolized bacteria to find niches to survive and create biofilms thus increasing the likelihood of spreading and contaminating products. A single factor ANOVA test revealed that the increase in population and time were related. Longer time could lead to the increase in bacteria populations in growing biofilms waiting to be re-aerosolized by processes like hosing down between morning and afternoon shifts.

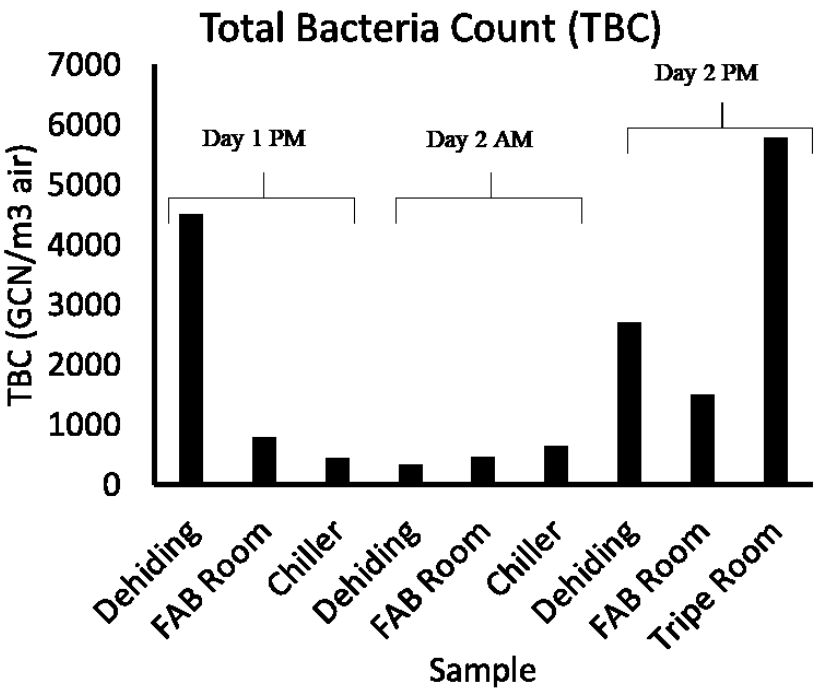
Total Bacteria Count (TBC)
TBC (GCN/m3 air)
7000
6000
5000
4000
3000
2000
1000
0
Day 1 PM
Day 2 AM
Day 2 PM
Dehiding
FAB Room
Chiller
Dehiding
FAB Room
Chiller
Dehiding
FAB Room
Tripe Room
Sample

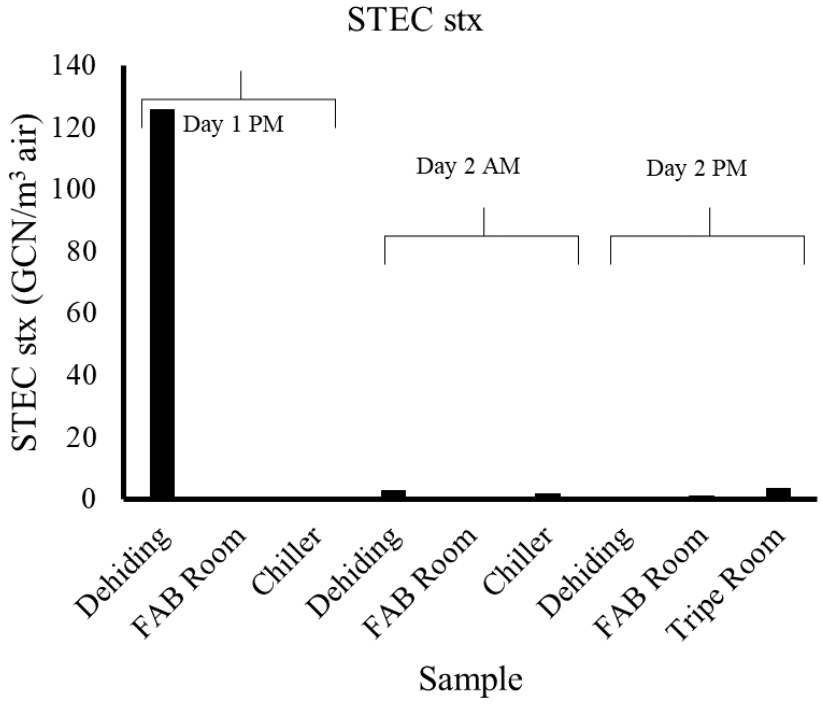
STEC stx
STEC stx (GCN/m3 air)
140
120
100
80
60
40
20
0
Day 1 PM
Day 2 AM
Day 2 PM
Dehiding
FAB Room
Chiller
Dehiding
FAB Room
Chiller
Dehiding
FAB Room
Tripe Room
Sample

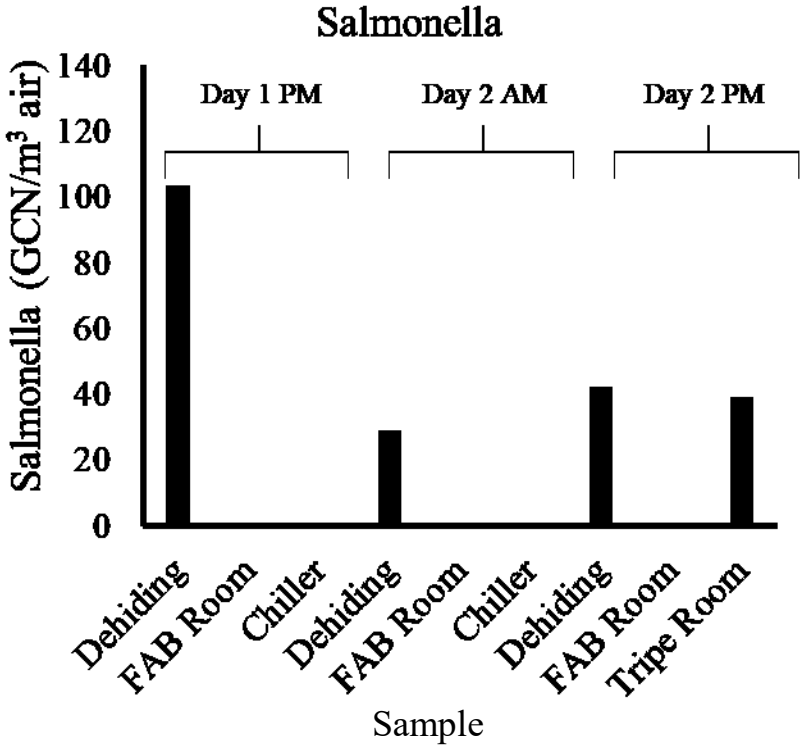

*Figure 3. TBC, STEC, and Salmonella collected in a two-day period separated between morning and afternoon. (Top) Total bacteria count based on the ribosomal 16S gene collected in the morning and afternoons at Facility A. Highest total bacteria counts in dehiding, tripe, and fabrication (FAB) rooms. (Middle) STEC quantitated based on the presence of Shiga toxin gene (stx). Elevated STEC stx in Dehiding (Day 1); Traces in chiller and FAB rooms both days; Tripe room (Day 2). (Bottom) Salmonella quantitated based on the presence of invasion gene (inv*A*). Highest Salmonella concentration (~ 40 GCN/m^3 air) in dehiding and tripe room on Day 2.*

Bacteria's growth rates have a strong relationship with temperature and relative humidity regarding to environmental stress factors. In order to acquire a stronger profile on the effects of relative humidity and temperature in a meat packing facility in regards to behavior with bioaerosols two HOBOs were placed next to the two continuous WWC running in the dehiding area and the fabrication room. The dehiding area is designed to be the dirtiest area of a meat packing facility while the fabrication room is supposed to be the

cleanest area. Within these two varying areas the environmental factors were analyzed to determine if they affected any outcome of the different bioaerosols that were inspected within the facility. The dehiding area has two major makeup air (MUA) units that are designed to blow air into the room with an outlet HVAC system that has the directional flow of clean air to dirty air. In Facility A's fabrication room the MUA unit is turned off to reduce safety hazards and health factors during the packaging process. The seasonal temperature and different controls of the HVAC system in the two rooms explain the different ranges of temperature and relative humidity found in Figures 4 & 5. As in dehiding area 1 it is common for heat to rise during the day with less control since the day starts off cooler in the spring. This shows an inverse relationship with relative humidity as temperature increases as the air becomes less saturated. Warmer air holds less water vapor, which acts as a transport for bioaerosols. In the fabrication room, since the water vapor content is constant throughout the day, as temperature decreases the more saturated the air becomes thus increasing the relative humidity. This can be a problem as biofilms can be formed easier, causing a higher concentration of contamination.

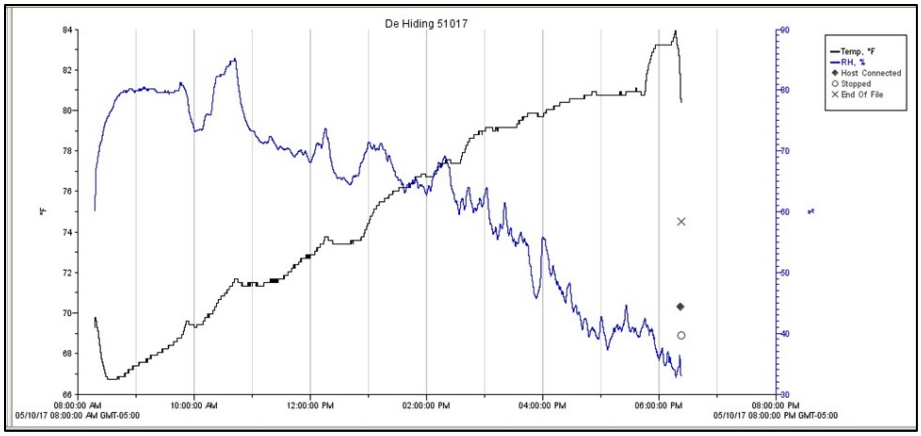

Figure 4. Temperature data collected by the HOBO Datalogger placed near WWC 1 location found in dehiding area 1. Relative humidity and temperature collected in the dehiding Area 1 (8:20am – 6:30pm), an inverse relationship can be found between the two properties. Temperature range: 67 ºF – 81 ºF and relative humidity range: 61% - 85% - 33%.

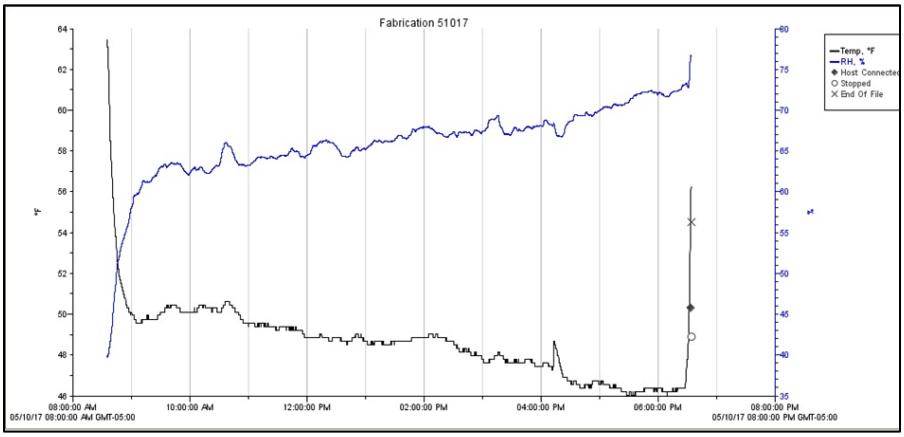

Figure 5. Temperature collected by the HOBO Datalogger placed near WWC 5 & 6 location found in the fabrication room. Relative humidity and temperature data for the fabrication room collected (8:30am – 6:30pm), an inverse relationship is shown with temperature and relative humidity. For the fabrication room standard USDA protocol is followed in monitoring temperature. Temperature range: 63ºF - 50ºF - 46 ºF and relative humidity range: 40 – 77%.

The microbiomes collected in the bioaerosol samples were analyzed by Illumina Sequencing for each sample location. Each WWC hydrosol sample was labeled with the location where the WWC was placed within the facility. In Table 1, the extracted sample

number, location, working time, and hydrosol collected show the difference in microbiome data i.e. how many different sequences (frequencies) were detected and how many are related to *Salmonella* and *E. coli*.

Table 1. Illumina Sequencing of Spring DNA Data Set Acquired from 100 LPM WWC

Sample	Location	Sampling Time	Air collected (m^3)	Enterobacteriaceae Frequency (%)
1	Dehiding room (Day 1 PM)	9.30am-11am	9	1.04
2	Fabrication room (Day 1 PM)	7.30am-11am	21	0.79
3	Chiller (Day 1 PM)	7.50am-11am	19	0.64
4	Dehiding room (Day 2 AM)	11am - 6pm	42	0.48
5	Fabrication room (Day 2 AM)	11am - 6pm	42	0.41
6	Chiller (Day 2 AM)	11am - 6pm	42	1.14
7	Dehiding room, dynamic sampling (Day 2 PM)	8:10am - 3pm	41	0.48
8	Fabrication room, Dynamic sampling (Day 2 PM)	3pm - 6pm	18	0.47
9	Tripe room (Day 2 PM)	1:00pm - 6pm	30	0.36

Dynamic sampling under the location indicates that the WWC was moved during the collection period to cover the full area of the room. The Illumina sample files were processed using QIIME 2, an open-source bioinformatics pipeline for performing microbiome analysis from raw sequencing data. The bacterium was broken up into kingdom, phylum, class, order, family, genus, and species. Some of the Illumina Sequencing files were missing scientific classification details. A missing detail found in the data set was for both *Salmonella* and *E. coli*. These were only broken up to their order, Enterobacteria, upon following classification the family of these both as well are Enterobacteriaceae, in which they separate by genus (52, 53). In this paper Enterobacteriaceae will be assumed to include *Salmonella* and *E. coli* when analyzing the QIIME data. Many Enterobacteriaceae are categorized as pathogens in humans/animals or phytopathogens which are economically devastating. Thus, even with this broad classification these bacteria are to be avoided in meat processing facilities. The DNA sequence can be further analyzed based on more specific sequences, to identify more specific genera.

Ultimately the Illumina Sequencing analyzed by QIIME 2 was to confirm the qPCR data for the Spring hydrosol samples. Though looking at both percentages, Enterobacteriaceae frequency and the percentage of bacterial classifications (STEC *stx* count added with *Salmonella* count, divided by TBC per location), they did not match up exactly. The qPCR detected more bacteria in the WWC hydrosol samples than the sequencing. This difference in amount of bacteria could be due to bacteria that were not identified in the Illumina Sequencing. In percentages, there is a range of 47-91% between

these samples in which the sequence data only could determine frequencies as either *bacteria* or *unassigned*. This large discrepancy could explain why the Enterobacteriaceae frequency is by a tenth lower in fraction compared to the qPCR data. Moreover, the trends in percentages did not entirely match either for the processes. The major discrepancies can be found for both the fabrication room and chiller room. There is no relation between the TBC count and the total number of frequencies found for each location. Though comparing the TBC figure values to the values in Table 1, the trends seem to stay relatively true, except for discrepancies in the fabrication room and the chiller room.

Summer Facility A qPCR Analysis

The second data set of bioaerosols were collected in the summer over a one day sampling period, similarly to the spring sample set, ultimately broken up into the morning and afternoon times of the day. The bioaerosols collected were categorized into Total Bacteria Count (TBC), STEC *stx*, STEC *eae,* and *Salmonella.* In this data set the introduction to test for STEC *eae* primer was introduced, as *eae* is more of a precursor to the detection of *E. coli*. The samples collected were further separated into the time of collection, the day sample was taken, and location within the facility. The four data sets of GCN/m^3 values for the air samples collected were calculated and plotted (Figure 6). CFU related to cubic meter (m^3) air was calculated to analyze the number of viable bacteria in each location. The increase of TBC, Salmonella, STEC *stx* can be determined by the difference in time, air volume, and total volume of hydrosol collected for each sample. For TBC the highest counts were found in the dehiding room with 1.18 x 10^7 GCN/ m^3 in the morning and 1.46 x 10^7 GCN/m^3 in the afternoon. This is to be expected as the dehiding

area should be the most contaminated area as the dehiding process and the hide should carry the most bacteria found in a meat packing facility. Due to the WWC operation, different locations were conducted at different times seen below. The next highest bacteria count was found in the tripe room at 30,000 GCN/m^3. Both collections present significant evidence that bacteria can be found throughout the facility. There was no significant trend ($P<0.5$) between morning and afternoon with the TBC. *Salmonella,* STEC *eae*, and STEC *stx* were all detected with lower GCN/m^3 counts in the morning and later found at higher concentrations in the fabrication room by the afternoon. For *Salmonella* 1,800 GCN/m^3 was found in the morning with increasing levels in the afternoon to 3,100 GCN/m^3. The fabrication room showed counts of 460 GCN/m^3 while there were no counts in the morning. This trend can be seen in STEC *eae* though there are no counts found in the dehiding location in the afternoon, but found increasingly in the fabrication room by 1,200 GCN/m^3. High counts of STEC *stx* were found in the dehiding area at 2,00 GCN/m^3 and later found in a clean location, the chiller, with 200 GCN/m^3. This can be inferred as a suboptimal HVAC design in the facility. With the increasing number of cattle heads being introduced in the facility, the dehiding counts increased, resulting in more dirty air moving to the clean areas in Facility A.

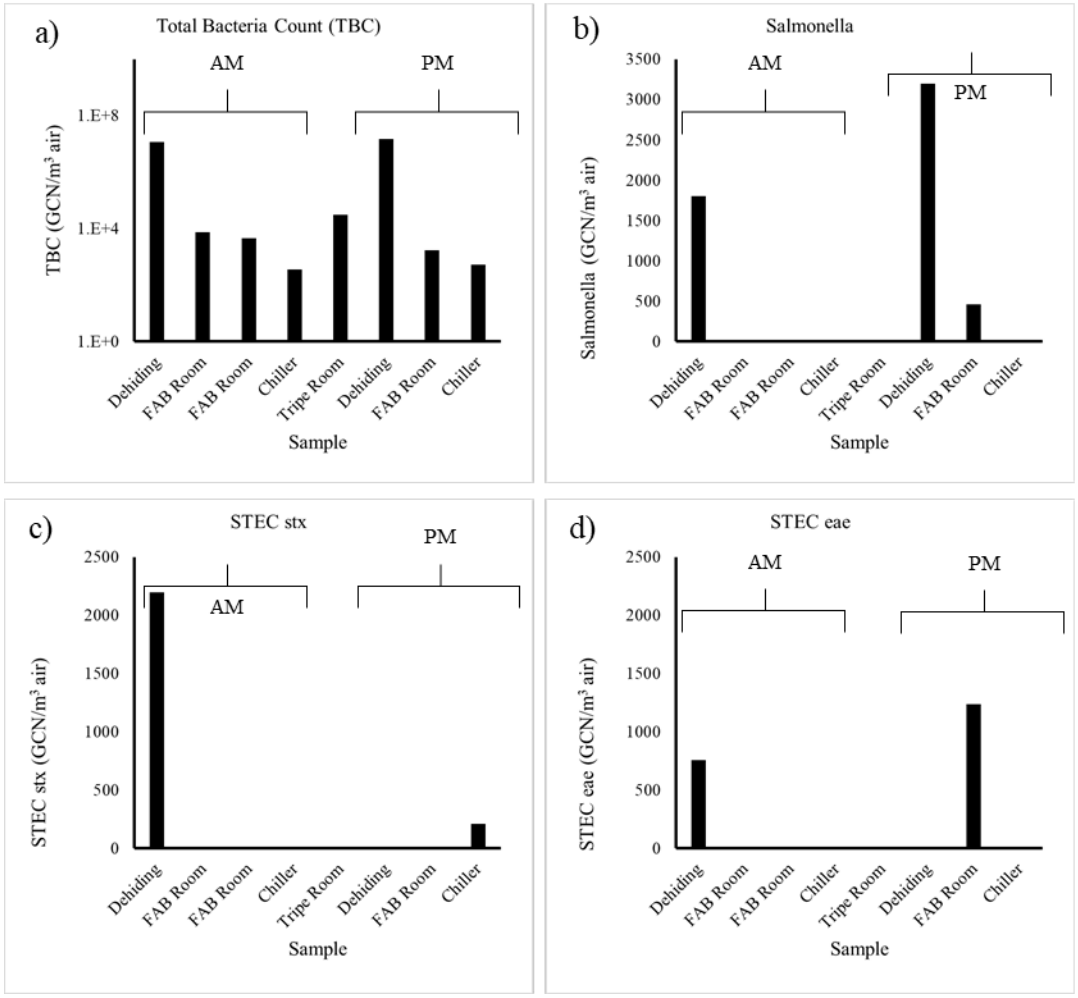

*Figure 6. TBC, Salmonella, STEC stx, and STEC eae samples collected in the summer, broken up between morning and afternoon. (a) TBC based on the ribosomal (16S) gene calculated on a logarithmic scale. Dehiding room stayed constant throughout the day with the highest total count. Other sample locations increased as the day progressed. (b) Salmonella based on the invasion gene (inv*A*) increased exponentially into the afternoon and was also detected in the afternoon. (c) High counts of STEC based on the Shiga toxin gene (stx) found in the morning, while in the afternoon found in the chiller. (d) Highest counts of STEC based on intimin adherence gene (eae) found in the afternoon in the fabrication room. Overall by the afternoon pathogens spread to chiller and FAB room. Tripe room was tested all day.*

HOBO Dataloggers were again placed in the dehiding area and the fabrication room next to the WWC. Due to the seasonal change each of these rooms needs to be

monitored with different parameters than in the spring. Since Facility A must keep the regulations not exceeding 85ºF, the temperature relationship is more drastic than that of the spring comparing Figure 7 to Figure 4. This could be an explanation as to why there were higher counts in summer than in the spring due to the increase of water vapor in the air. In Figure 7. This relationship can be seen in Figure 8, as the relative humidity can only reach a certain level in the fabrication room until the USDA needs to intervene. To intervene, they increase the temperature thus providing a better environment for bacteria. Towards the end of the day in the fabrication room, the two relationships moved closer which could explain why the fabrication room provides a better environment for bacteria to grow in the afternoon.

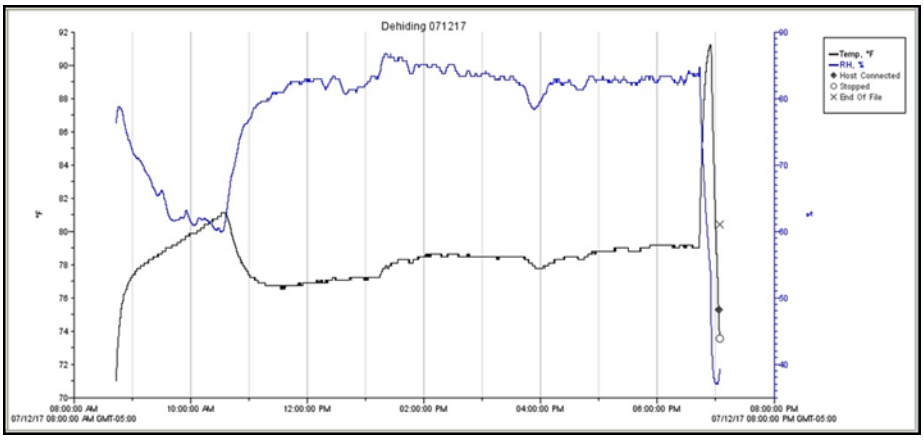

Figure 7. Temperature collected by HOBO placed near WWC 1, in summer, found in dehiding area 1. Relative humidity and temperature were collected in the dehiding area 1 (8:40am – 7pm), due to higher temperatures in the summer, dehiding room must be cooled once reaching a certain temperature. Temperature range: 71 ºF – 81 ºF – 78ºF and relative humidity range: 78% - 60% - 84%.

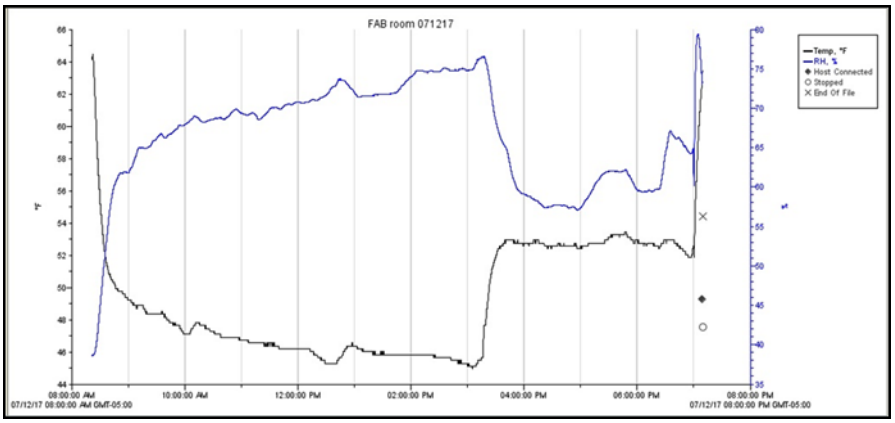

Figure 8. Temperature collected by HOBO placed near WWC 5 & 6 location, in summer, found in fabrication room (WWC was moved from location 5 to location 6 by the afternoon). Relative humidity and temperature were collected in the fabrication room (8:20am – 7pm), location 6 showed a closer relationship between the two. Temperature ranges: 63°F - 45°F - 53 °F and relative humidity ranges: 38 – 76 – 64%.

The ranges were broken up and averaged to find a correlation between temperature and the change in relative humidity. The values between temperature and relative humidity are not much difference in the overall average between the spring and summer data set. Most changes between the two seasons can be found in a time-step scale. Different temperatures and relative humidity are reached at different times of the day. This aspect of the meat packing facility can be looked further into with more sampling days to characterize the temperatures reached during the spring and summer months. Though the different cycling of temperature and relative humidity on bacterial colonies can be further investigated to determine the most optimal growing conditions. Though it is well known that the summer months allow more bacterium to be introduced into facilities due to prior increase of concentration in hides of cows at hotter temperatures and with higher humidity. Comparing the difference in time steps it can be seen that the crossover in Figure 4 to the

inverse relationship between temperature and relative humidity occurs much later in the day in the dehiding room in the spring season. The crossover occurs during 2 PM, while in the summer the dehiding room crossover occurs a little over 10 AM. This increase of relative humidity can be seen as a quality control problem introducing more of a bacterial concentration. This can be directly seen viewing both Figures 3 and 6 as there is a substantial increase in sample numbers (TBC, STEC *stx*, and *Salmonella)* for the dehiding room. As well this relationship is seen in the fabrication room. Though the crossover of the inverse relationship between temperature and relative humidity occurs in the same time step, in the summer months relative humidity reaches higher levels. When this aspect is lowered due to facility protocol the temperature has to be increased in the production room which can reactivate bacteria that were once dormant. If the bacteria are no longer dormant in a larger area it is more likely that an outbreak can occur. Using ANOVA testing these environmental factors show a relationship with the change of concentration levels between the two sampling periods. Though there is a change in relationship, controlling relative humidity and temperature in this large area can be extremely hard especially when facilities need to meet USDA regulations.

To quantify the bioaerosol samples collected in the summer, qPCR, Illumina Sequencing and analysis using QIIME 2 was performed following the same procedure as in the spring. The WWC hydrosol sample results are shown in Table 2. The same assumptions for the frequencies categorizing *E. coli* and *Salmonella* with Enterobacteriaceae were made for the summer DNA samples as well. There was a larger range in the total number of frequencies from the summer season to the spring season.

This can conclude that the total number of frequencies this does not entirely describe the level of contamination of bacterium.

Table 2. Illumina Sequencing of Summer DNA Data Set Acquired from 400 LPM WWC

Sample	Location	Sampling Time	Air collected (m^3)	Enterobacteriaceae Frequency (%)
10	Dehiding room (AM)	8am-12.30pm	27	0.005
11	Fabrication room, Dynamic sampling (A-AM)	7.35am-12.30pm	29.5	0.02
12	Fabrication room, Dynamic sampling (B-PM)	12.30pm-1:30pm	12	0.12
13	Chiller (AM)	7am-12.30pm	33	0.45
14	Tripe room (AM&PM)	8.15am-2.30pm	25.5	0.48
15	Dehiding room (PM)	2pm-6pm	24	0.11
16	Fabrication room (PM)	2pm-6pm	24	0.15
17	Chiller (PM)	1pm-6pm	30	0.71

Dynamic sampling indicated under the location only occurred in the fabrication room between the AM and PM period to cover the whole area of the room. Using QIIME 2 the

summer sequencing frequencies found in Table 2 were compared to that of Figure 6. Comparing the Enterobacteriaceae frequency ratio to the percentage of classifications found in the qPCR sample did not match up exactly similar to the spring data set. These trends show discrepancies with the fabrication room, tripe room, and chiller locations. The magnitude of the factors as do not correspond to the qPCR analysis either. In this data set, there was a percentage range of 46 – 99% between these samples in which the sequence data could only determine frequencies as either unassigned or general bacteria. Similarly, to the spring data, this could explain why the qPCR does not match in trends or magnitude. Again, there is no relation between the TBC and the total number of frequencies found in each location. Comparing Table 1 and Table 2 there is no correlation in temperature change or relative humidity and the increase in the total number of frequencies. Moreover, there is no trend in the difference of the total number of frequencies with the volume of air collected per location. On average looking at just Enterobacteriaceae frequency % the spring samples seem to have more Enterobacteriaceae DNA. Though in the summer DNA sequence analysis there is a higher mode percentage that locations have 90% above unassigned frequencies. Further investigation of the bacteria that are not assigned should give more detail and accuracy to the quantification of the qPCR samples.

Shown in both Figure 6 and Table 2 there is a concentration increase from the morning sampling period to the afternoon sampling period. Looking closely into Figure 6, the increase can be seen in total bacteria and all cases of the different bacterial indicators. In the TBC graph, there is an increase in bacterial concentration in the dehiding room and chiller. With the qPCR analysis it can be seen that there are higher counts/detection of

Salmonella in the dehiding room by the afternoon. As well there is a higher concentration in the fabrication room in the afternoon compared to the morning. For STEC *stx* there is a detection in the dehiding room in the morning, then the appearance of this toxin in the chiller in the afternoon. For STEC *eae* there is detection in the morning in the dehiding room with an appearance in the fabrication room in the afternoon. This could indicate migration throughout the day due to improper HVAC flow and properties that are not being exchanged enough to expel these bioaerosols. This migration can be verified through QIIME 2, as these frequencies of the same strand can be seen through analyzing the magnitude of frequency. In Table 2 the magnitude of frequency is seen to increase with Enterobacteriacae strands from morning then to the afternoon. There is a significant increase in magnitude with the time change. As the temperature increases in the fabrication room by the afternoon with relative humidity being high for most parts of the day, this combination leads to an excellent environment for bacteria to travel and grow. Further analysis will be done to determine if the type of strains found in the morning is the same as the strains found in the afternoon. This would prove their migration and that HVAC is a larger issue to be examined in meat packing facilities.

Original HVAC Facility Design

The flow trajectory of the room is created including the entry room/knocker, dehiding areas, chiller, tripe Room, and fabrication room. Making up of 6 major intakes, including the Makeup air units (MUA) ranging from 50,000-55,000 cfm and 27 exhausts: ranging from 3,000-25,000 cfm. The original HVAC design for Facility A is to push clean air right before the fabrication room through the chiller into the dehiding areas. This would

make the flow circulate from clean to dirty areas to reduce the spread and movement of bioaerosols. Figures 9-12 show the CFD model of Facility A with the flow trajectory displaying for both spring and summer's velocity mapping. Since there was no remodeling of the facility or HVAC the flow trajectory should not have changed between the months. The fluid type used a predefined air provided by SolidWorks Flow, with a specific heat ratio of 1.399 and molecular mass of 0.0638 lb/mol. The temperature and humidity are not far off in deviation in the behavior to change the fluid dynamics of the building for modeling purposes. An average of the temperature and relative humidity were made between the spring and summer samples. The temperature for the environmental profile was 61.91 ˚F with a relative humidity of 64.51%. The temperature and humidity should only affect the bacterial viability and concentration in the pre-harvesting process.

The initial flow of the facility starts at the MUA unit near the knocker which introduces dirty air into the facility as air directly hits cattle coming into the facility. The cattle arrive with dirty hides from pre-harvesting and get hosed off which allows bacteria to be aerosolized easier. The surrounding outlets do not match the inlet flow volume flow rate allowing the bioaerosols to form and spread throughout the facility. Bioaerosols will always be present in the dirty areas of the facility so this area is not of emphasis on stopping decontamination especially in large facilities. From following the flow, it can be seen that dehiding area 2 contains corners and narrow hallways that introduce eddies creating larger, more frequent vortices to form. This formation leads to an increase in the contamination of bioaerosols that allows biofilms to grow easier. Due to the circulation air that circulates throughout the facility, it can be seen that the air is being pushed in the

chiller where the bacteria are dormant until reaching the production room. The WWC placement within the facility was at locations where vortices are not established well enough for the air draft from the HVAC system to be in direct contact. This would allow a non-bias for the data sample acquired as well as displaying the regular movements of travel with bioaerosols. This type of migration can be seen especially in Figures 10 and Figure 11, these two represent where and what type of bacterium was found in the spring and summer data set. The type of bacteria is represented by color and placed in the room location where it was found. The size of the indicator is related to the amount of concentration found in that room quantified by the qPCR earlier. In Figure 10. it can be seen that all bacterial genes (*Salmonella inv*A, STEC *stx,* STEC *eae)* originated in the dehiding room where each migrated to different rooms at different concentrations. This could be due to the HVAC set up of the facility which allows the migration of bioaerosols to occur. Though the time separation between the two data sets is months it can be seen that all three indicator genes start at the dehiding room. Traveling along into the tripe room (in the spring instances) they are taken through the dehiding area 2. In both data sets *Salmonella* was found in the chiller rooms in which the fabrication room showed all the bacteria were found originally in dehiding room. Through standard USDA protocol, these bioaerosols should have been stopped at the chiller room where it is indicated by yellow lines where the start of the clean area begins in the facility. This migration of air could only be due to improper HVAC design and the lack of performance in air exchange rates within the facility in the dirty areas.

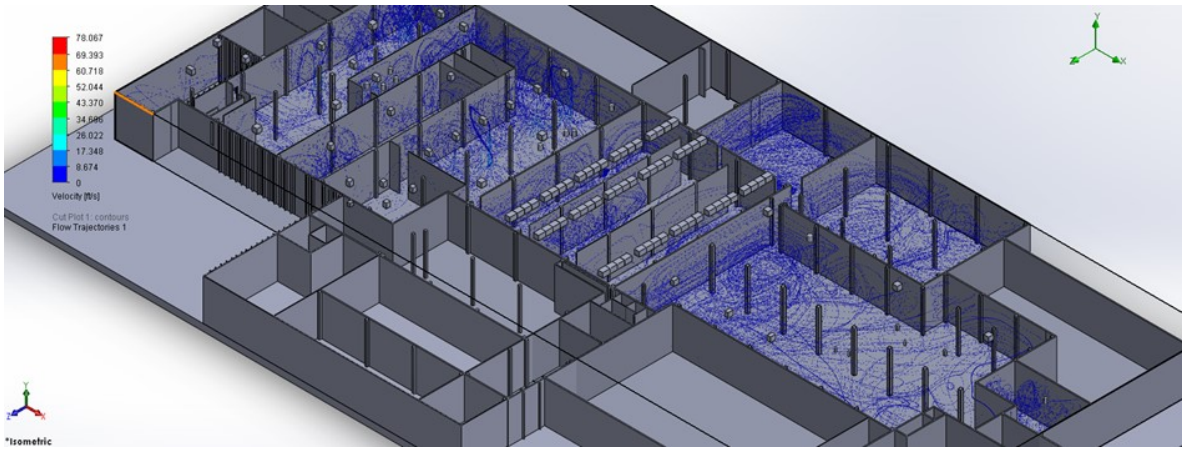

Figure 9. Isometric view of Facility A displayed in SolidWork Flow Analysis. Displaying flow trajectory of Facility A set by original HVAC inlets and outlets.

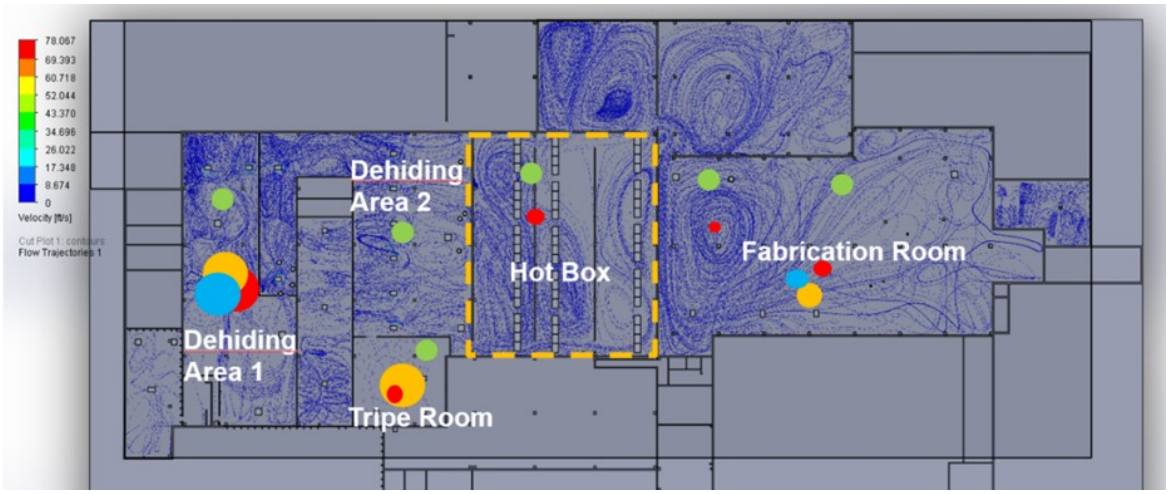

Figure 10. Top view of flow trajectory in Facility A created by intake and outtake values premeasured in an HVAC assessment. Major vortices form around corners and through narrow hallways and entryways throughout the facility. Air becomes well mixed except in stagnant areas inside Chiller and Fabrication room. Yellow lines surrounding Chiller indicate the beginning of the clean section of the facility. Green dots indicate the WWC locations placed in the facility, Spring pathogens are indicated by dot and size: yellow - Salmonella invA*; red - STEC stx (toxin gene); blue - STEC eae (intimin gene).*

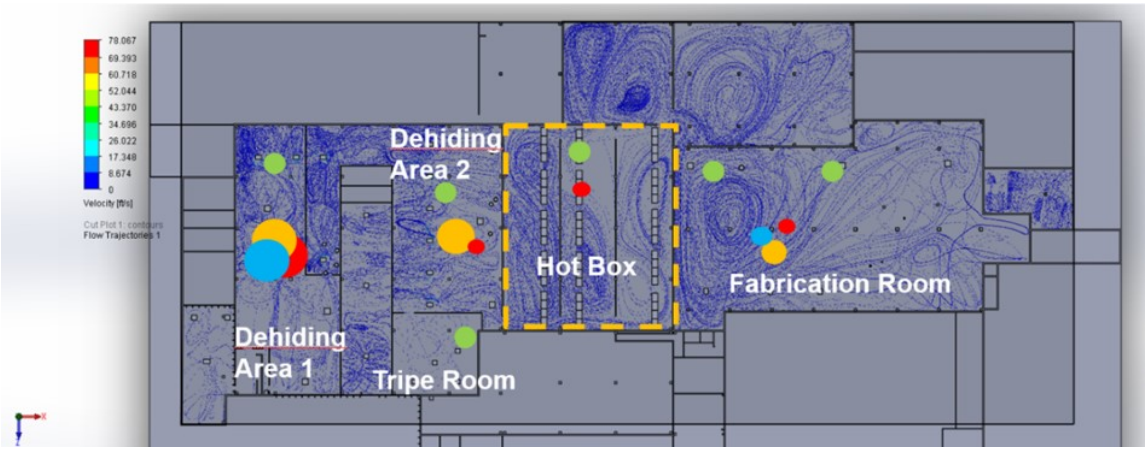

Figure 11. Top view of flow trajectory in Facility A with simulation ran and dots indicating the difference in pathogen from spring to summer. Summer pathogens are indicated by dot and size: yellow - Salmonella invA*; red - STEC stx (toxin gene); blue - STEC eae (intimin gene).*

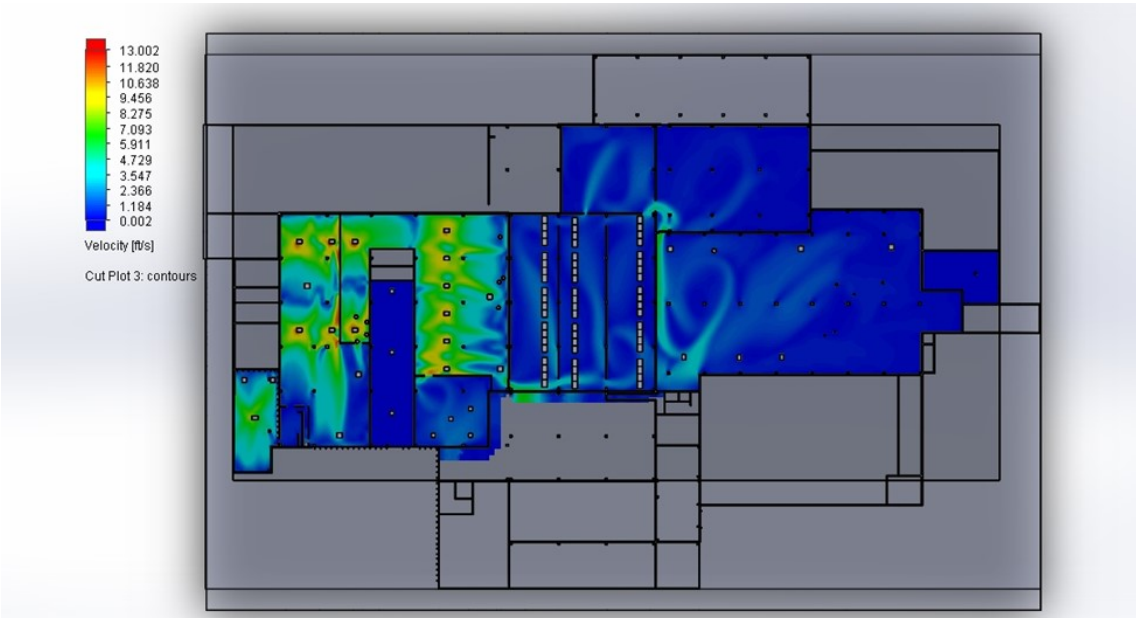

Figure 12. Top view of velocity gradient map of Facility A with original HVAC design.

With the accumulation of vortices seen around dehiding areas one and two, it can be determined that when new air is introduced entering the chiller of the facility there is an increased likelihood that this will be contaminated air. As contaminated air enters the

chiller the cold temperature of the room can lead to bacteria mechanizing to be dormant until temperatures are then reached where they can grow again, like in the fabrication room. Between the two rooms that are separating the chiller and fabrication room a lot of swirling and vortices are created due to the narrow hallways. Figure 12 shows a contour mapping of solely the HVAC velocity movement within the facility. The color gradient shows how exactly the concentration of velocity moves throughout the facility. The dehiding areas have the highest level of velocity magnitude which would propel the bioaerosols to move towards the clean air of the facility. Narrow doorways and tight corners restrict in area of movement which increases the velocity introduced from open areas to narrower corridors. With the reintroduction of more intakes from MUA units in the dehiding area, the velocity gradient will further increase. Since this area needs more circulation and air exchanges due to regulation it does introduce powerful air drafts into clean areas.

The fabrication room only has exhaust units that produce a positive pressure room system when reaching this area. This interaction of velocity air movement can also be related to the LMA, describing the latency of air in the facility. Since both entrances and exits of these rooms are so small, the air is seen circulated longer in these two rooms thus raising concern in concentration especially in the first room, seen in Figure 13, displaying a longer local mean age of air. The first room takes 4 times longer (~2,200 seconds) to change out air while the second room connecting to the fabrication room takes 6 times longer (~3,300 seconds) compared to the dehiding room (~550 seconds). Air forms major vortices near the entrance of the fabrication room where LMA in this area is slowed down.

As the latency decreases throughout the facility due to the processes of production, the clean areas will have more particles deposition. This is the same location where the carcasses are being brought in by the chain link system thus also where the bioaerosol attachment and impact can occur on the product. Though more air changes are needed in the dirty areas this pattern should be kept throughout the facility in order to decrease contamination.

Since the MUA is off during operational hours there is no introduction of new clean air in the fabrication room only the exhausts and the flow of air coming from the Chiller. This way the chiller is the only room being introduced to dirty air with a higher deposition that could lead to a higher risk of contamination. In studies researching air emissions in meat packing facilities, it was determined that beef cattle emit about 6.2 Log CFU AU^{-1} h^{-1} of Enterobacteriaceae, where AU is denoted by animal units, approximately 500 kg of animal weight (54, 55). With the average cow weighing about 1,200 lbs this accounts to 14.88 Log CFU per hour from a single head. About 1800 cattle go through a day, dividing the cattle equally per shift this would be approximately 900 heads in 5 hours. This equals about 180 head per hour which equates to 2,678.4 Log CFU in an hour which is emitted from cattle alone to be filtered out. There is not enough outtake to draw in the bioaerosols or enough intake to separate vortices and flow through the contaminated air.

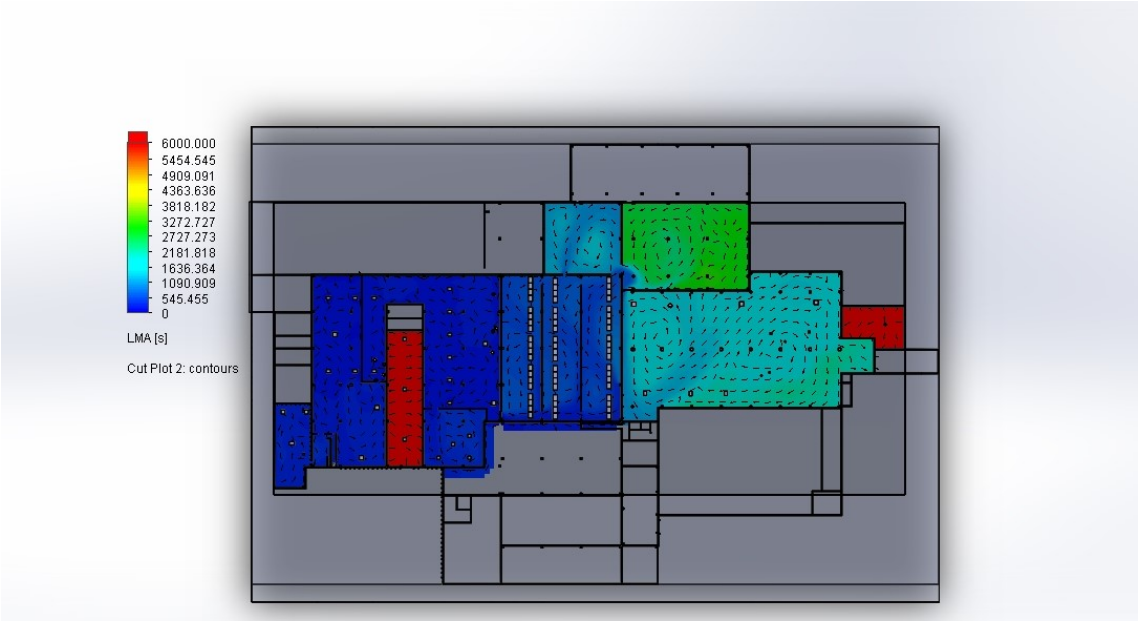

Figure 13. Local mean age of air with original HVAC facility design. Black arrows display the vector direction of the overall air movement within Facility A.

New Air Mitigation Solution

The difficulty of adding inlets and outlets to a running Facility A could slow down production or halt it all together for weeks if it disturbs the main production line. Financially for a company this is not feasible. Thus, a solution was created in order to mitigate the risk of contamination by bacteria being entrained in the air involving the HVAC design of the facility. The mitigation design implemented in the system was a cold room air curtain, modeled after a standard industrial model. The air curtain will be placed right above the two entryways of the cleanest rooms of the facility the chiller and the fabrication room. The air curtain will run at a speed at 5 ft/sec at a height of 12 – 13 ft running on a 1 horsepower motor. Since the unit only takes 1 hp this would make the energy use for the air curtain low and cost the facility financially less, compared if an

outbreak were to occur. Most industrial air curtains are priced between $800-1,500 per unit. The average maintenance costs for a conventional air curtain is around $0.02 per square meter. For the entire facility, this comes out to only $48.28/year of maintenance costs, which is very low for both air curtains. Air curtains lower fuel costs for a room without climate separation, with air curtains costing $0.87 per square meter of room, and standard systems costing $1.45 per square meter of room. This attributes to an annual fuel savings cost difference of $3,500 for the whole facility in a year. Compared to recall costs which can range from a hundred thousand to a million dollars this cost is very low.

This solution was tested first in SolidWorks Flow to understand the flow trajectory that will be introduced solely by the air curtain if introduced in Facility A. Shown in Figures 14 and 15 the air curtain flow from the chiller entrance splits into two creating a curtain between the dehiding area 2 exit and the chiller entrance, indicated by the green circles. The air that travels through the chiller which should be significantly cleaner will influence the air now flowing into the fabrication room. With the second air curtain in front of the fabrication room, this would allow the second mode of protection in the cleanest parts of the facility. As the air curtain pushes the air faster through in a laminar flow it is breaking up vortices created by the narrow corners. Solely from the air vectors that both air curtains created it can be seen that the velocity travels at a low rate in the range of 5-9 ft/s depending on the area of travel. An air curtain creates a barrier between two rooms and almost seals them by directing the flow down. This will dictate the room flow as the original flow will not penetrate as much through into other rooms. The pressure balance and initial flow of the room will also affect the efficiency of the air curtain flow

will. Figures 14 and 15 show that the air curtain blends naturally with the flow of the original HVAC. The red arrow vectors represent the clean air coming back and circulating into the clean air which will break up the concentration of biooaerosols. Though vortices are still created due to the design of the facility these will not introduce biofilms since the air will be filtered through the machine system.

Shown more in Figure 16, the original HVAC trajectory is blended with the air curtain trajectory. Displayed by the blue vector arrows the original flow trajectory of the entire system is seen to be influencing more the flow of the air curtains trajectory. This allows more clean air to mix within the facility thus breaking up the production of biofilms where bioaerosols can impact. Moreover, fewer vortexes are formed throughout the facility and at the entrance of the fabrication room where major turbulence was detected earlier through CFD analysis. In the dehiding room 1, the clean air created from the air curtain in front of the chiller is mixing with the original HVAC air. As the original HVAC flow allowed bioaerosols to flow through the facility this mixture should reduce their concentration. This mixture is seen as well all through dehiding room 2. With the introduction of the new air curtain HVAC flow, the original HVAC flow penetrates the barrier more towards the bottom of the curtain. This would make the contaminated air deposit on the floor where it will be harder for the bacteria to aerosolize. With the original HVAC air that penetrates through it can be seen that right after the chiller a major vortex is created by contaminated air. The HVAC air curtain air traps the major vortex of contaminated air eliminating more contamination that could be introduced in the fabrication room. As it moves to the room right before the fabrication room more mixing

occurs within the room where air finally enters into the fabrication room. Though the air introduced by the air curtain moves much slower than the original HVAC system, it influences the air movement. This can be seen as the majority of the fabrication room contains flow originating from the air curtains.

Figure 17 like Figure 12 displays a velocity contour map of how the HVAC air curtain affected the overall velocity profile. The major difference between flows in comparison is that the velocity is raised to about 3 ft/s after the entrance of the chiller and fabrication room. This increase in velocity will push out the flow thus creating fewer opportunities for vortices to form. The bigger eddy seen from the original HVAC design is broken up and pushed more towards the back wall. As well it can be seen that the room right after the chiller has weakened the eddy in that room. As well the extra air intake is seen to increase the velocity of Facility A overall. This changed the latency of the air displayed in Figure 17. The new HVAC design did not change the LMA of the dehiding area which will be the base standard (~550 seconds). The biggest change can be seen though in the difference of factorization in LMA. In the room right, after the chiller the LMA speed is decreased only by a factor of two (~1,100 seconds), and the room right before the fabrication room went to a decreased factor of three (~1,650 seconds). As well the fabrication room increased to a slower LMA factor of just two. This major change in LMA would reduce deposition as a faster change of air is now introduced in the cleaner areas of the facility. In the fabrication room, an LMA gradient can be seen moving away from the air curtain. This would indicate that the air curtain did shorten the mean age of

air. Comparing the velocity vector arrows there is less of a circular pattern in Figure 17. This would conclude a better breakup of eddies that are introduced by turbulence.

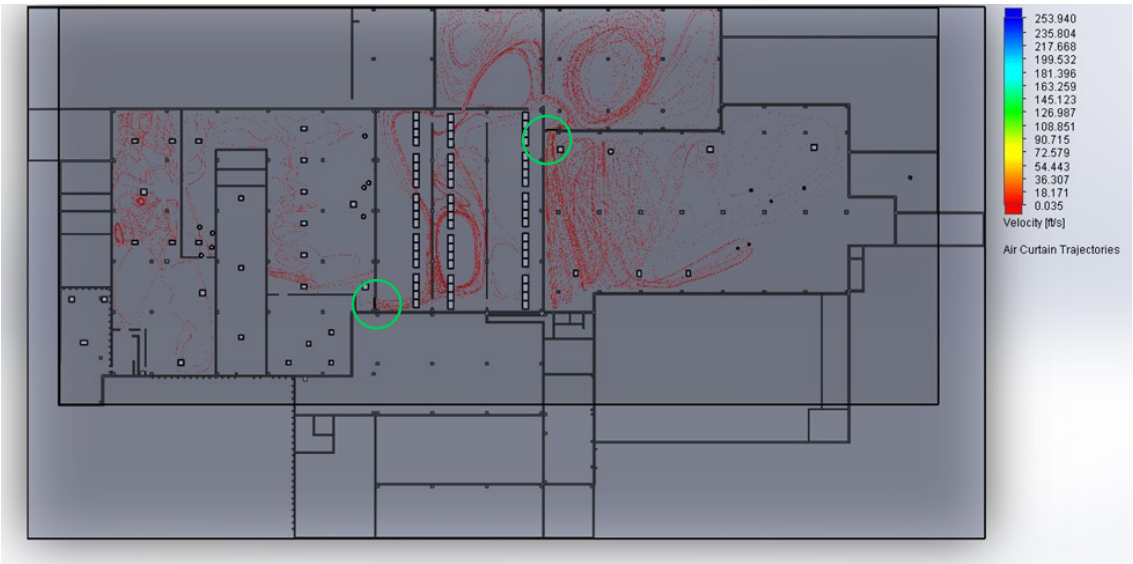

Figure 14. Top view of flow trajectory with the addition of two air curtains in Facility A. Air curtains are set as an inlet of 5ft/sec placed in-between entrances where high sanitation is needed. Air curtains are marked with a green ring where it is placed in the simulation.

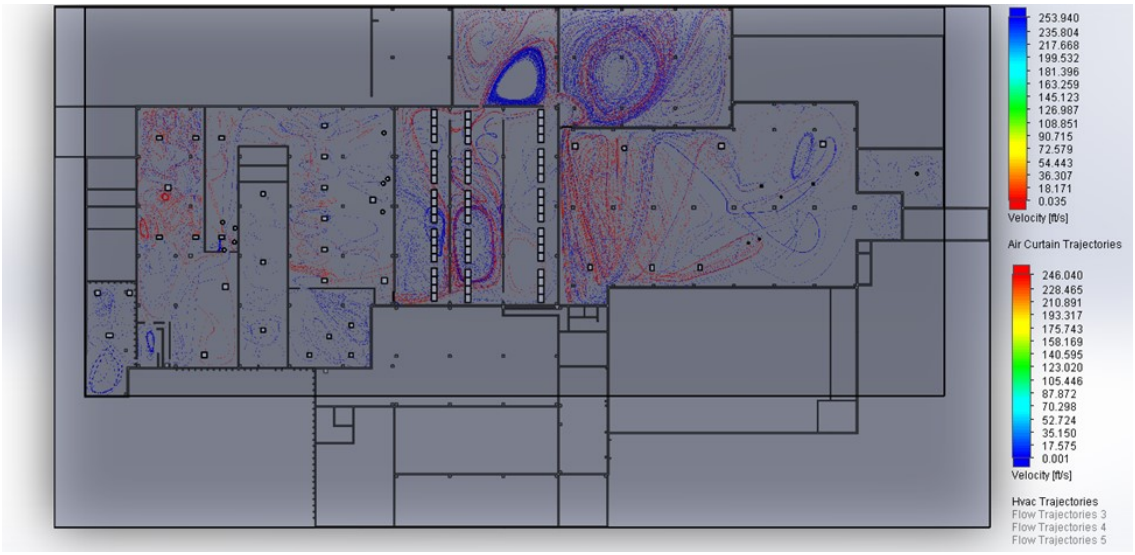

Figure 15. Top view of flow trajectory of original boundary layer inlet and outlets in addition to two air curtains in Facility A. Air curtains introduce clean air that dominates the chiller and fabrication room. Air curtain airflow trajectory is colored on an opposite spectrum from the HVAC airflow pattern.

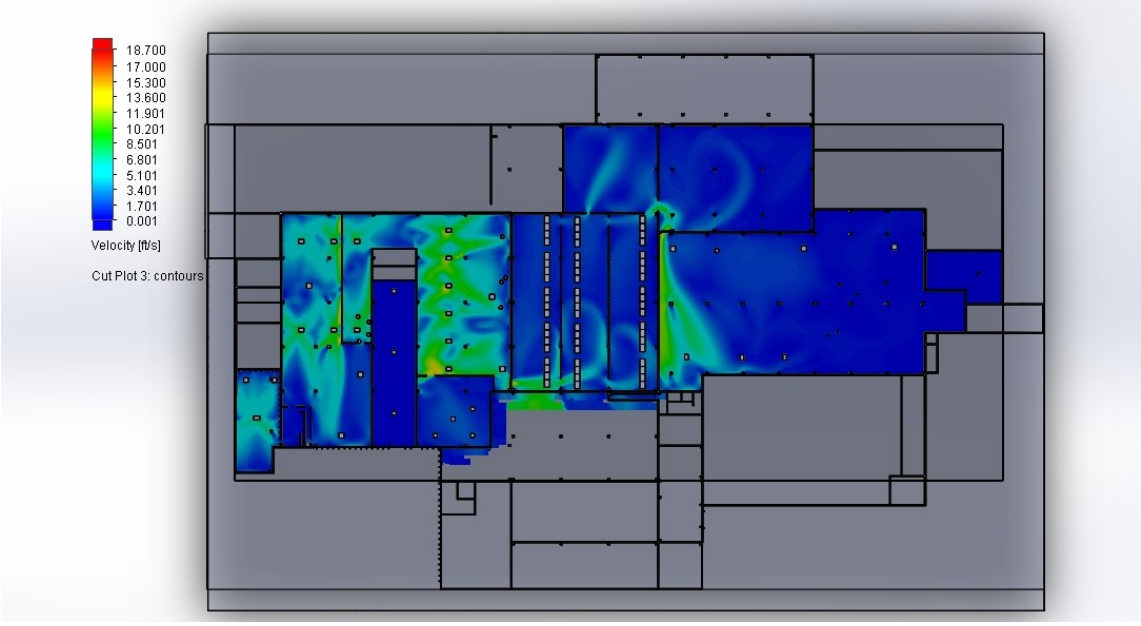

Figure 16. Top view of velocity gradient map of Facility A with the addition of two air curtains to the original HVAC design.

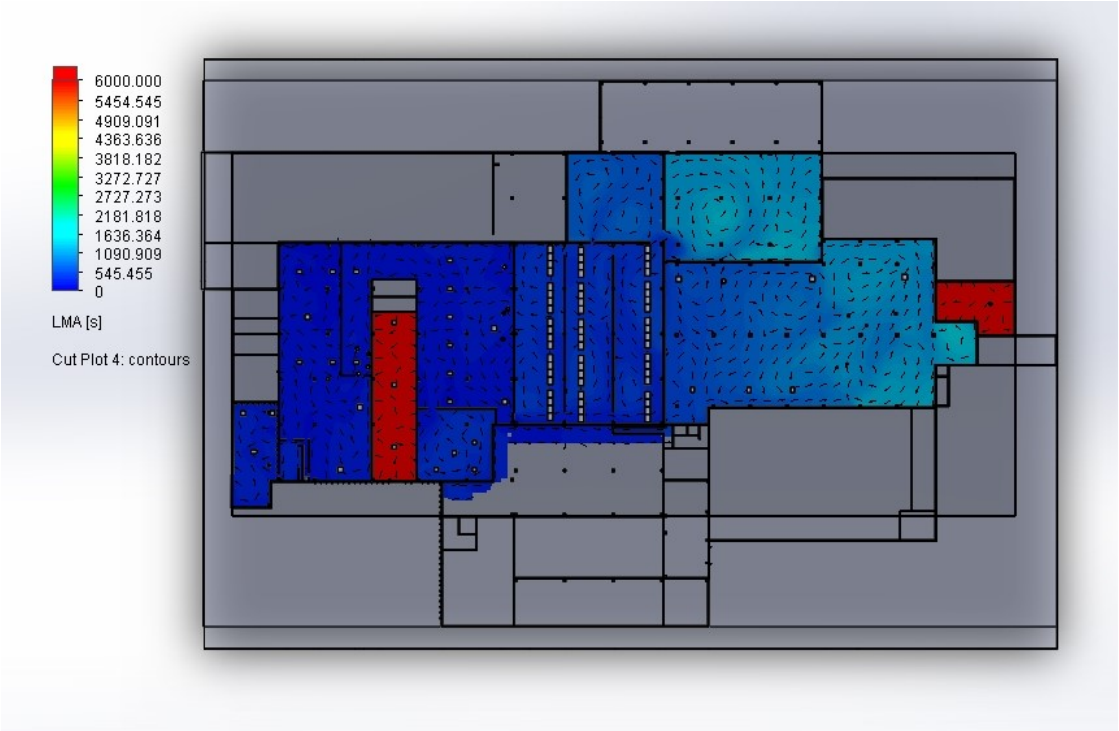

Figure 17. Local mean age of air with the addition of the two air curtains to the HVAC facility design. Black arrows display the vector direction of the overall air movement within Facility A.

To verify that the air curtain design would act the same way as in the CFD of Facility A, a chamber was replicated to act as if it was an entryway. The replica used an Awoco 24" Super Power 2 Speeds 800 CFM Commercial Indoor Air Curtain, (CE Certified 120V Unheated, with Easy-Install Magnetic Switch). This air curtain contains two speeds at 785 CFM and 628 CFM. In this study, the 628 CFM was used and tested to replicate closely to the airspeed used in the new HVAC design of Facility A. Though it does run a little higher than the exact speed that was modeled in the chamber replica CFD model. The dimensions of the intake of the Awoco 24" air curtain where air expelled was a 22.5" x 2.75" rectangle. These exact opening measurements were used in the CFD model

as well. Figure 18. shows the dimensions of the front of the chamber where the air curtain was installed. Since the air curtain was 10” in height a hole was cut in the ceiling and the air curtain was placed in the backing of the front wall. The direction and placement are applied in the CFD model.

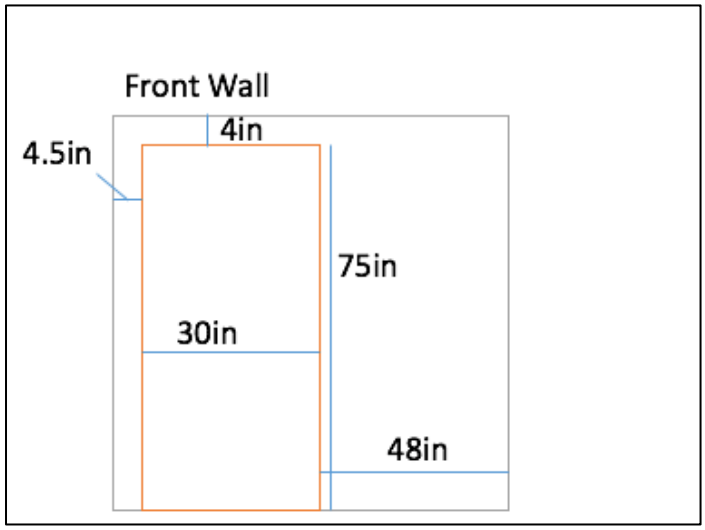

Figure 18. Dimensions of the front doorway used in the chamber design. These dimensions were used in the CFD air curtain chamber model.

In Figures 14-17 the air chamber design was seen to break up eddies, make a barrier between entryways/rooms, decrease LMA, and provide proper mixing of clean air. All these aspects are created when the velocity is increased by the air current and laminar flow patterns are introduced to help form and influence the original HVAC system. Stated in Beck et. al (2019), the ventilation design that displaced flow and created a shorter span of LMA increased the contamination removal effectiveness (CRE) in facilities. CRE can

be defined as the concentration of particles (in this case, bioaerosols) in the exhaust, then divided by the mean concentration in the given facility. In his study, the most optimal design to increase CRE was a ventilation system that shortened the flow isolating the contaminated air where the exhaust can collect the particles fast enough. Beck et al. created a ventilation system that expelled air closer to the ground to which would help push back and up the particles affected by convection. Hoods were included in the optimal design of the new HVAC system created in the study so that when objects produce heat (i.e. workers, machinery, or carcasses) which would trigger convection it would rapidly be expelled by the exhaust ports naturally. The majority of the HVAC design in Facility A has the exhausts in the ceiling already, shown in Figure 19. The air curtain velocity trajectory pushes the flow down from where it circulates back to be pushed down again. This motion is the same that was seen to increase the CRE without making major HVAC reconstruction.

Figures 19-21 show the CFD model of the replica of the chamber made to verify the behavior if installed in Facility A. In this model a pressure outlet was placed outside the chamber to demonstrate how the air curtain moves in a negative air pressure system. The chamber represents the area where passive airflow is moving out. Since the fabrication room only contains exhausts during operational hours this creates negative air pressure. The chiller room which is connected to the fabrication room pulls in the air since there is no intake for which to pull most from. The chamber then indicated the smaller corridors and entrances that is pulling its own intake enough to expel in the exhausts, but not enough to replace contaminated air entirely. This would create the effect of the air curtain's flow

to be pulled into the negative pressure room. It can be seen even though the air curtains main flow trajectory is being pulled this still creates a barrier where two separate eddies can be seen between the curtains. The wall is created by a higher velocity pushing away and fabricating the flow of air. This behavior is seen as well in Figure 14 when the flow is being pulled into the chiller and fabrication room.

In all three of these figures, the whole chamber and system were included in the model, but the area of focus was cropped to emphasize the behavior the air curtains created. In Figure 20 a top view of the air curtain flow demonstrates that even though it has a rectangular shape as an inlet there is higher velocity expelled in the middle of the air curtain that spreads out in a gradient away from the center. Since there are higher speed and concentration of velocity from the air curtain it is important to measure an air curtain in the exact length of the doorway as well as to align the centers together. This would create the best barrier in HVAC flow. As air is expelled out the linear vectors from the air current velocities are hitting the floor directly. The blue curved arrows indicate the recirculated air. It can be seen that there are two distinct pathways created by this barrier. Figure 21. shows the decrease of velocity in the z-direction. A downward plume is created where the flow follows the shape of the room back to the top of the air curtain. This shows how in Facility A the circulated air will filter through the top, if not filtered this would also help migrate the particles to the top where the exhaust is located. This would also push the particles downward to faster deposition and away from the clean areas which increased CRE in the rooms (Beck et al., 2019). These movements validate the same actions that are occurring in the new HVAC CFD model.

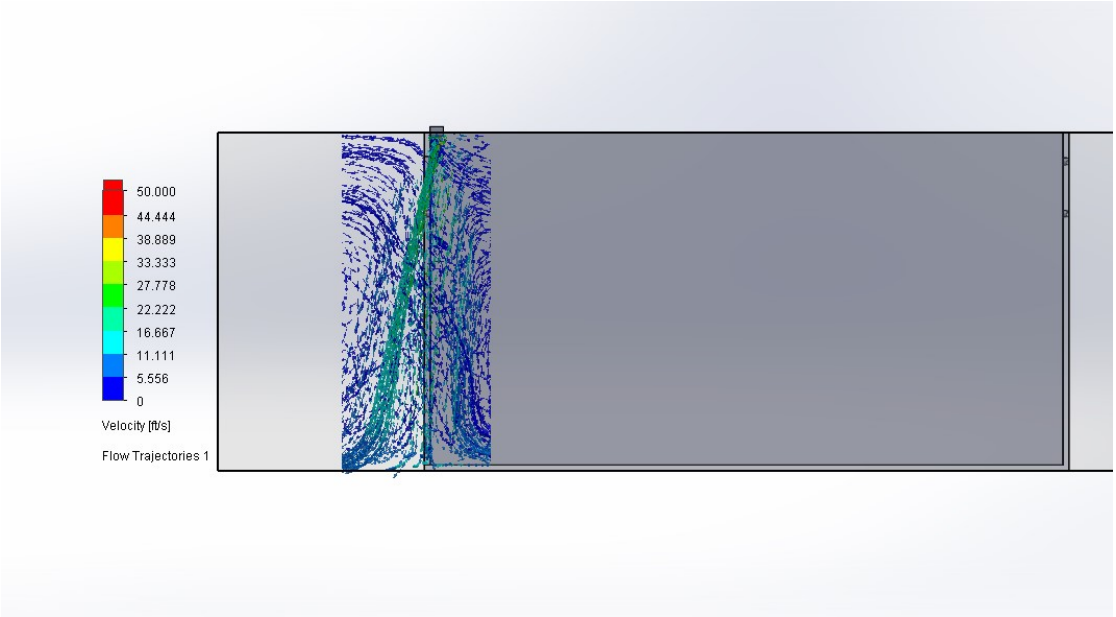

Figure 19. Side view of CFD air chamber model. A section of the CFD model was focused in order to show the area of importance in movement. The darker area indicates the inside of the chamber area while the light grey box indicates the outside area.

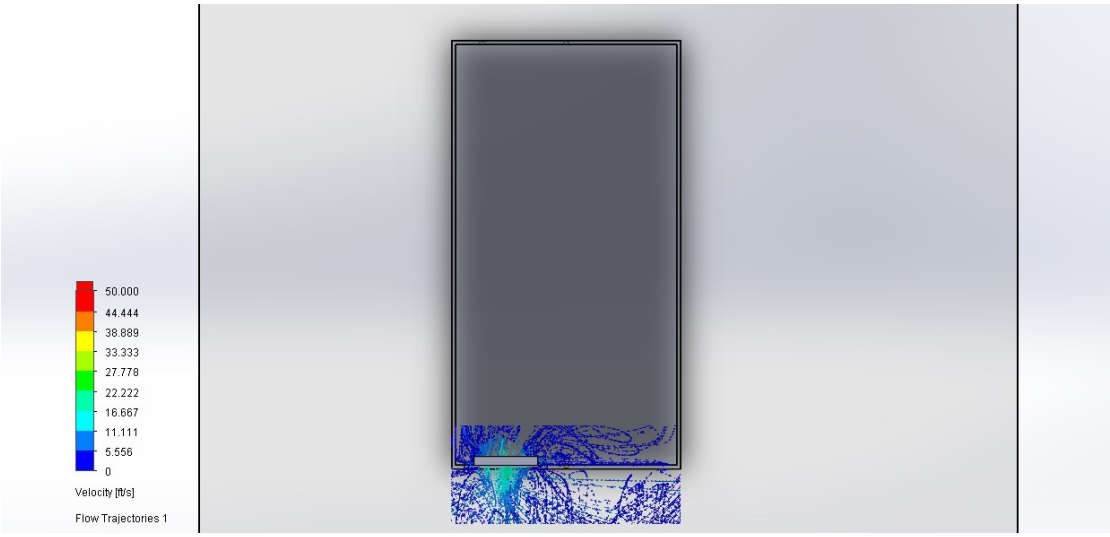

Figure 20. Top view of CFD air chamber model.

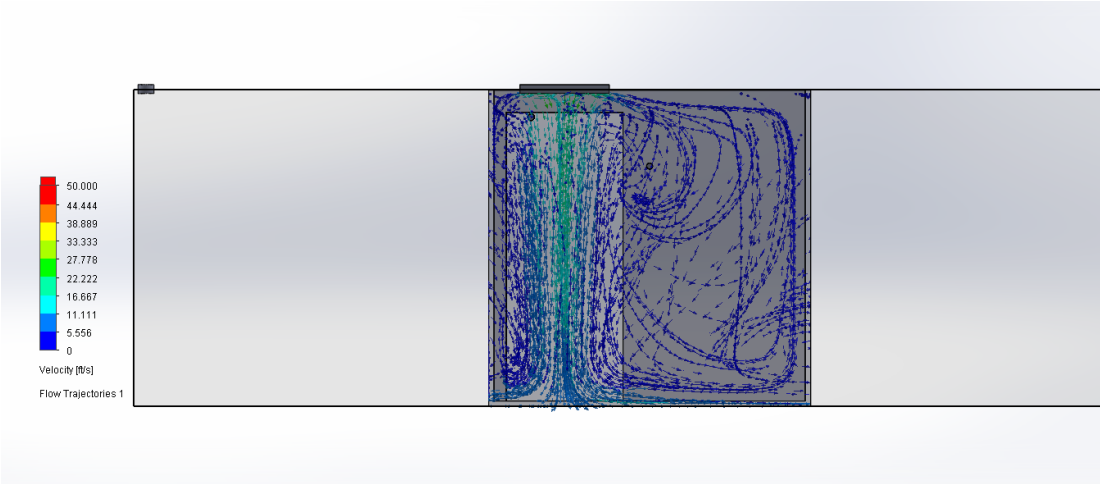

Figure 21. Front view of CFD air chamber model.

To validate the CFD model a replica of this chamber was made where an anemometer was used to measure the velocity range in the x, y, and z-direction. The data points were collected in 3 rows in the y-direction. The row points started 5 inches away in the x-direction of both sides from the center of the air curtain inlet. In the y-direction starting from the middle of the door the other two row data points were 14 inches away from the center. This would then create 6 equidistant rows of the air curtain dimensions. These 6 rows, then in the z-direction with the first point starting 16 inches from the bottom going up 16 increments thus measuring up to the top height of the door. A stand was used with the anemometers in order to establish stability in the measurement. These heights will be indicated through alphabetical order of A-E, with A being the first 16 inch starting point. The rows go in order from left to right in numerical order 1-3. This area covered is seen in Figure 20. the top view of the chamber. Where the 5.56 ft/s range reaches the outer corners and the 22 – 17 ft/s range found in the room outside the chamber. Thus creating

all together 30 data velocity points, 15 points in the inside of the chamber and 15 points outside in the room. Each point was measured three times then averaged to get a statically correct data set, shown in Table 3 and Table 4. The environmental conditions of the CFD model were the same as the chamber used in Facility A. Viewing the tables these points match the velocity gradient created in the CFD model by location. Seen in Figure 22 and Figure 23 the difference in velocity points are seen. On average of each velocity data points in each set there is a 15-20% inaccuracy of data points. Discrepancies in the data could be due to the anemometer measurement errors when recording. As well it could be that the air curtain is not producing fully developed laminar flow standard to its performance error/capability. This same range in velocity with both model and empirical data set shows the accuracy of the CFD model. To increase the accuracy of the empirical data measurement 3D ultrasonic anemometers should be used. This accuracy can conclude the accuracy of the new HVAC Facility A model.

Table 3. Inside Velocity Data Points of the Air Curtain Replica

Z-direction row	Column 1 (ft/s)	Column 2 (ft/s)	Column 3 (ft/s)
E	5.2152	10.9716	4.7232
D	3.9852	8.2656	3.1488
C	3.6408	3.936	1.1808
B	1.3776	2.706	1.6236
A	2.0664	2.46	1.6728

Table 4. Outside Velocity Data Points of the Air Curtain Replica

Z-direction row	Column 1 (ft/s)	Column 2 (ft/s)	Column 3 (ft/s)
E	17.056	24.46	4.3132
D	5.1824	25.748	1.8204
C	17.384	16.564	4.92
B	10.168	10.496	5.084
A	6.068	10.496	4.1

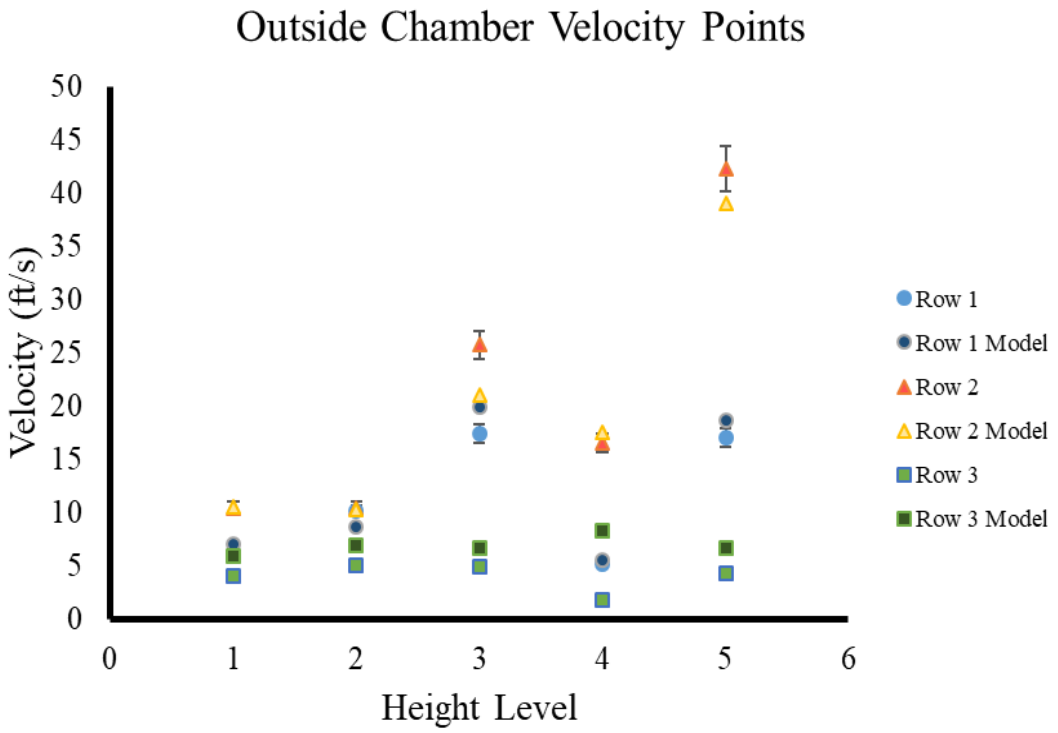

Figure 22. *Comparison of velocity data ponts of the outside chamber. Each row is described by the shape of the marker. Row represents the recorded velocity data point from the experimental chamber. Row model represents velocity data points take from the CFD model. Error bars represent anemometers 5% range of error.*

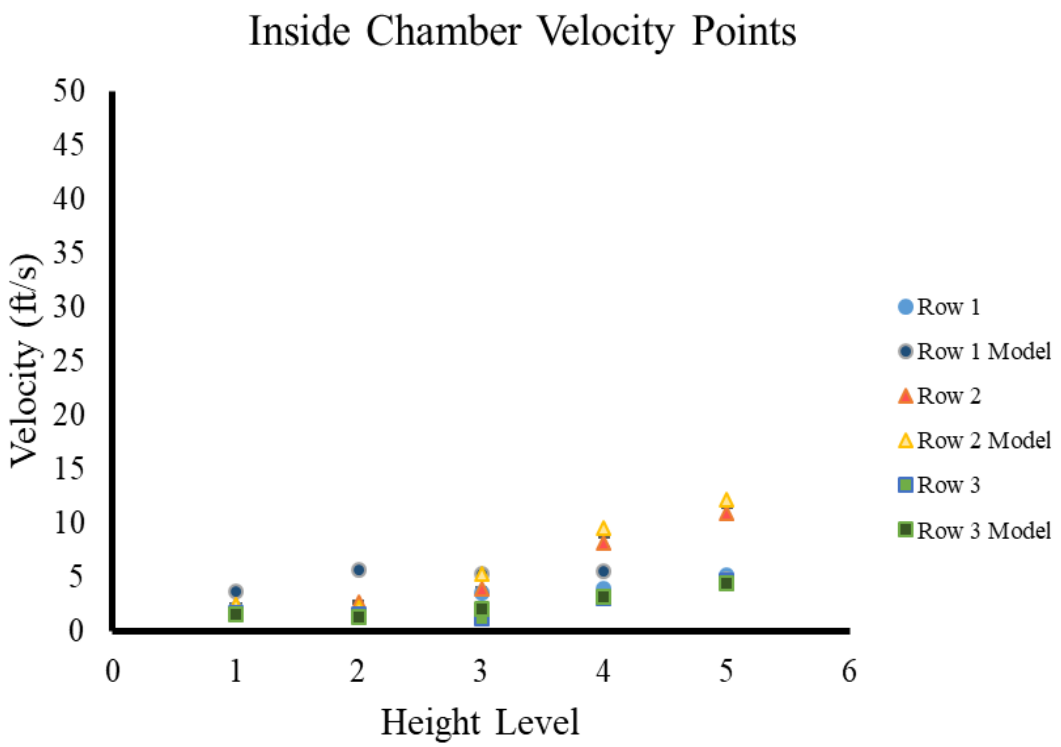

Figure 23. Comparison of velocity data ponts inside of the chamber. Each row is described by the shape of the marker. Row represents the recorded velocity data point from the experimental chamber. Row model represents velocity data points take from the CFD model. Error bars represent anemometers 5% range of error.

CHAPTER V

CONCLUSION

The purpose of the study was to assess the environmental and working conditions of a large scale meat packing facility through dynamic air sampling and airflow modeling. Ultimately to develop and create a solution to mitigate bioaerosol spread. Focusing on HVAC design, an air curtain was installed as a mitigation technique to redirect the airflow of the facility. Incorporated into the study was a CFD analysis to understand how flow patterns could affect aerosolized particles. Paired with these two techniques an enumeration of the total concentrations of bioaerosols in different locations of the facility was accomplished. Using WWC collectors it was concluded that high concentration bioaerosol collection was dependent on the physical location of the slaughtering process. Another factor that affected the process was the airflow behavior of that area. As well it could be that the concentration of bioaerosols was seasonal and time dependent. In agreement with many studies there was a distinct seasonal difference between the two sampling periods during spring and summer within the counts in total bacteria, *Salmonella,* and STEC found in Facility A. Upon inspecting the two seasons, a higher concentration was found in the summer time compared to the spring. In the spring data collection, the highest concentrations of TBC were found in the dehiding area with 4,500 GCN/m^3. In the summer in the same area, TBC was found to be 1.18 x 10^7 GCN/m^3. Similarly, for *Salmonella* the spring counts were only 43 GCN/m^3 while in the summer

they were 3,100 GCN/m^3. This result shows how temperature and relative humidity affect the optimal growth and spread of bioaerosols.

WWC collection was broken up into two parts of the day during the aerosol collection based on time. The facility worked in two time periods: morning rotation, broken up with a complete hosing of the dehiding area and activation of the HVAC system in the fabrication room, followed by the afternoon rotation. When the afternoon rotation began the HVAC system in the fabrication room was turned off again like in the morning. Following the time scale of collection comparing morning concentration and afternoon concentration, it can be seen that there is an increase of concentration in the afternoon and migration of contamination found in "clean" areas that did not have a trace of bioaerosols in the morning. This shows that the hosing process does not properly remove particles. In fact, this could help aerosolize unwanted bacteria that were later found in the chiller and fabrication room. Looking at the summer sets it was seen specifically with *Salmonella* as lower counts were found in the morning and then higher in the afternoon, also detected later in the FAB room. The movement of aerosolized bacteria through the HVAC system can be seen with the qPCR quantitation for both primers sets of STEC (*stx* and *eae*). Bacteria were found in high counts in the morning, 2,200 and 780 GCN/m^3, respectively. No STEC were detected in the afternoon, however, higher counts were found in the clean facility area. STEC *eae* was found with higher counts than in the dehiding area with about 1,200 GCN/m^3. Through the CFD analysis it can be seen that the HVAC design helps direct the air from the dehiding area to the clean areas, emphasizing the importance of how HVAC design needs to be taken into larger consideration when building meat processing

facilities. Further analysis using Illumina Sequencing would help identify the microbiome and verify the quantity of bacteria from qPCR. The Illumina Sequencing data processed through QIIME 2 displayed the frequencies of Enterobacteriaceae found traveling through the facility from the morning to the afternoon shift. This frequency concentration quantifies the concentration assessed through qPCR. The movement and the mechanism involved are visually displayed through the original HVAC CFD model.

The placement of the two air curtains was designed to help mitigate the influence of bioaerosol spread within the facility through its HVAC system. The comparison of the original model HVAC design and the new model HVAC design shows that with the installation of air curtains the airflow would be broken up, reducing the areas where vortexes formed heavily. As well the curtains would act as a barrier to the clean areas that were affected throughout the day and during the cleaning process in the midday shift at the facility. The design positively affected the velocity contours profile throughout the facility, decreased the LMA in different rooms, and reduced turbulence in large eddy areas. These factors all contribute to the deposition and collection rate from the exhausts. Following studies previously done before these factors increase the CRE of Facility A. The air curtain attached to the chamber representing the room to corridor connection in Facility A empirical data showed accuracy to the CFD model. Due to time constraints of installing the air curtain in Facility A in the spring of 2020, the chamber method of verification showed the accuracy of real life studies to SolidWorks Flow modeling. As this modeling was deemed accurate within an acceptable error range, it can be inferred

that the new HVAC air curtain design would introduce factors that would reduce bioaerosol concentration and movement.

Further studies should include campaigns of experimental field testing where a whole week of collection could occur. This would allow more statistical results supporting the data set and show clearer relationships throughout the week. These campaigns should also take place in other seasons such as fall and winter to complete the data set found in this study which only has spring and summer. Temperature and relative humidity data should also be collected outside while it is collected inside. This would be beneficial to the theory of how there is a seasonal influence on the spread and increase in bioaerosols. To further enhance the study more WWC should be placed throughout the facility to get more of an accurate analysis to the exact location where the influence of concentration can be found. This would help the analysis of larger rooms where bacteria concentrations are more focused on like in the fabrication or dehiding room. Further studies in different locations of larger meat facilities would also help develop a larger and broader trend in order to make a template for all large scale facilities. Understanding the temperature profile of a different facility in a different environment would explore the effect of temperature and relative humidity on bioaerosols. It would also result in more data points and spectrum of occurrence/trend related to one facility vs. another. A sampling campaign should be performed once the air curtain solution is installed to show the direct results of the mitigation solution.

REFERENCES

1. Omer MK, Alvarez-Ordonez A, Prieto M, Skjerve E, Asehun T, Alvseike OA. A systematic review of bacterial foodborne outbreaks related to red meat and meat products. Foodborne pathogens and disease. 2018;15(10):598-611.

2. Mead PS, Slutsker L, Dietz V, McCaig LF, Bresee JS, Shapiro C, et al. Food-related illness and death in the United States. Emerg Infect Dis. 1999;5(5):607-25.

3. Eisel WG, Linton RH, Muriana PM. A survey of microbial levels for incoming raw beef, environmental sources, and ground beef in a red meat processing plant. Food microbiology. 1997;14(3):273-82.

4. BARKOCY-GALLAGHER GA, ARTHUR TM, RIVERA-BETANCOURT M, NOU X, SHACKELFORD SD, WHEELER TL, et al. Seasonal Prevalence of Shiga Toxin–Producing Escherichia coli, Including O157:H7 and Non-O157 Serotypes, and Salmonella in Commercial Beef Processing Plants. 2003;66(11):1978-86.

5. Law JW-F, Ab Mutalib N-S, Chan K-G, Lee L-H. Rapid methods for the detection of foodborne bacterial pathogens: principles, applications, advantages and limitations. Front Microbiol. 2015;5:770-.

6. Nyachuba DG. Foodborne illness: is it on the rise? Nutrition reviews. 2010;68(5):257-69.

7. McFarland AR, Haglund JS, King MD, Hu S, Phull MS, Moncla BW, et al. Wetted Wall Cyclones for Bioaerosol Sampling. Aerosol Science and Technology. 2010;44(4):241-52.

8. Kulkarni P, Baron PA, Willeke K. Aerosol measurement: principles, techniques, and applications: John Wiley & Sons; 2011.

9. Collins LR, Keswani A. Reynolds number scaling of particle clustering in turbulent aerosols. New Journal of Physics. 2004;6(1):119.

10. Hussein T, Dada L, Juwhari H, Alfaouri D. Characterization, Fate, and Re-Suspension of Aerosol Particles (0.3–10 μm): The Effects of Occupancy and Carpet Use. Aerosol and Air Quality Research. 2015;15:2367-77.

11. Nazaroff WW. Indoor bioaerosol dynamics. Indoor Air. 2016;26(1):61-78.

12. Cox C. Physical aspects of bioaerosol particles. Bioaerosols handbook. 1995:15-25.

13. Scott E. Food Safety and Foodborne Disease in the 21 st Century. Canadian Journal of Infectious Diseases. 2003;14:277-80.

14. Dungan RS. BOARD-INVITED REVIEW: fate and transport of bioaerosols associated with livestock operations and manures. Journal of animal science. 2010;88(11):3693-706.

15. Altekruse S, Cohen M, Swerdlow D. Emerging foodborne diseases. Emerging infectious diseases. 1997;3(3):285.

16. Tenover FC. Mechanisms of antimicrobial resistance in bacteria. The American journal of medicine. 2006;119(6):S3-S10.

17. Davey ME, O'toole GA. Microbial Biofilms: from Ecology to Molecular Genetics. Microbiology and Molecular Biology Reviews. 2000;64(4):847-67.

18. Giaouris E, Heir E, Hebraud M, Chorianopoulos N, Langsrud S, Moretro T, et al. Attachment and biofilm formation by foodborne bacteria in meat processing environments: causes, implications, role of bacterial interactions and control by alternative novel methods. Meat Sci. 2014;97(3):298-309.

19. Burmolle M, Webb JS, Rao D, Hansen LH, Sorensen SJ, Kjelleberg S. Enhanced biofilm formation and increased resistance to antimicrobial agents and bacterial invasion are caused by synergistic interactions in multispecies biofilms. Appl Environ Microbiol. 2006;72(6):3916-23.

20. Brooks JD, Flint SH. Biofilms in the food industry: problems and potential solutions. International Journal of Food Science & Technology. 2008;43(12):2163-76.

21. Millner PD. Bioaerosols associated with animal production operations. Bioresour Technol. 2009;100(22):5379-85.

22. Gallagher MJ, Vaze N, Gangoli S, Vasilets VN, Gutsol AF, Milovanova TN, et al. Rapid Inactivation of Airborne Bacteria Using Atmospheric Pressure Dielectric Barrier Grating Discharge. IEEE Transactions on Plasma Science. 2007;35(5):1501-10.

23. Dirks BP, Dobrynin D, Fridman G, Mukhin Y, Fridman A, Quinlan JJ. Treatment of raw poultry with nonthermal dielectric barrier discharge plasma to reduce Campylobacter jejuni and Salmonella enterica. Journal of food protection. 2012;75(1):22-8.

24. Rengasamy A, Zhuang Z, BerryAnn R. Respiratory protection against bioaerosols: literature review and research needs. American journal of infection control. 2004;32(6):345-54.

25. Park J-H, Yoon K-Y, Kim Y-S, Byeon JH, Hwang J. Removal of submicron aerosol particles and bioaerosols using carbon fiber ionizer assisted fibrous medium filter media. Journal of mechanical science and technology. 2009;23(7):1846-51.

26. Brady-Estévez AS, Kang S, Elimelech M. A single-walled-carbon-nanotube filter for removal of viral and bacterial pathogens. Small. 2008;4(4):481-4.

27. Upadhyayula VK, Deng S, Mitchell MC, Smith GB. Application of carbon nanotube technology for removal of contaminants in drinking water: a review. Science of the total environment. 2009;408(1):1-13.

28. Xu Z, Shen F, Chen Q, Tan M, Yao M. Bioaerosol Science, Technology, and Engineering: Past, Present, and Future. Aerosol Science and Technology. 2011;45:1337-49.

29. King M, R. McFarland A. Bioaerosol Sampling with a Wetted Wall Cyclone: Cell Culturability and DNA Integrity of Escherichia coli Bacteria2011.

30. Hinds WC. Aerosol technology: properties, behavior, and measurement of airborne particles: John Wiley & Sons; 1999.

31. Hubbard JA, Haglund JS, Ezekoye OA, McFarland AR. Liquid Consumption of Wetted Wall Bioaerosol Sampling Cyclones: Characterization and Control. Aerosol Science and Technology. 2011;45(2):172-82.

32. Marshall WA. Laboratory evaluation of a new aerobiological sampler for use in the Antarctic. Journal of Aerosol Science. 1997;28(3):371-80.

33. Crook B, Sherwood-Higham JL. Sampling and assay of bioaerosols in the work environment. Journal of Aerosol Science. 1997;28(3):417-26.

34. Gan G, Awbi HB. Numerical simulation of the indoor environment. Building and Environment. 1994;29(4):449-59.

35. Gilani S, Montazeri H, Blocken B. CFD simulation of stratified indoor environment in displacement ventilation: Validation and sensitivity analysis. Building and Environment. 2016;95:299-313.

36. Yang L, Ye M, he B-J. CFD simulation research on residential indoor air quality. Science of The Total Environment. 2014;472:1137-44.

37. Katz A, Sankaran V. Mesh Quality Effects on the Accuracy of CFD Solutions on Unstructured Meshes. 49th AIAA Aerospace Sciences Meeting including the New Horizons Forum and Aerospace Exposition. Aerospace Sciences Meetings: American Institute of Aeronautics and Astronautics; 2011.

38. Driss D, Driss Z. Numerical simulation and experimental validation of the turbulent flow around a small incurved Savonius wind rotor. Energy. 2014;74:1 Pages 506–17.

39. Hathway EA, Noakes CJ, Sleigh PA, Fletcher LA. CFD simulation of airborne pathogen transport due to human activities. Building and Environment. 2011;46(12):2500-11.

40. Hussein T, Kulmala M. Indoor Aerosol Modeling: Basic Principles and Practical Applications. Water, Air, & Soil Pollution: Focus. 2007;8:23-34.

41. Shale K, Lues JFR. The Etiology of Bioaerosols in Food Environments. Food Reviews International. 2007;23(1):73-90.

42. Inc I. An Introduction to Next-Generation Sequencing Technology. 2016.

43. King MD, McFarland AR. Bioaerosol sampling with a wetted wall cyclone: cell culturability and DNA integrity of Escherichia coli bacteria. Aerosol Science and Technology. 2012;46(1):82-93.

44. Hoeksma P, Aarnink AJA, Ogink N. Effect of temperature and relative humidity on the survival of airborne bacteria= Effect van temperatuur en relatieve luchtvochtigheid op de overleving van bacteriën in de lucht. Wageningen UR Livestock Research; 2015. Report No.: 1570-8616.

45. Lam C, Bremhorst K. A modified form of the k-ε model for predicting wall turbulence. 1981.

46. Beck S. ZA, Castillo A., Maestre J., King M. . Computational Airflow Modeling Based on Pathogen Tracking at Food Processing Facilities 2018.

47. Rahn K, De Grandis SA, Clarke RC, McEwen SA, Galan JE, Ginocchio C, et al. Amplification of an invA gene sequence of Salmonella typhimurium by polymerase chain reaction as a specific method of detection of Salmonella. Molecular and cellular probes. 1992;6(4):271-9.

48. Rutherford ST, Bassler BL. Bacterial quorum sensing: its role in virulence and possibilities for its control. Cold Spring Harb Perspect Med. 2012;2(11):a012427.
49. VanGuilder HD, Vrana KE, Freeman WM. Twenty-five years of quantitative PCR for gene expression analysis. BioTechniques. 2008;44(5):619-26.

50. Faulkner WB, Memarzadeh F, Riskowski G, Hamilton K, Chang C-Z, Chang J-R. Particulate concentrations within a reduced-scale room operated at various air exchange rates. Building and Environment. 2013;65:71-80.

51. Faulkner WB, Memarzadeh F, Riskowski G, Kalbasi A, Ching-Zu Chang A. Effects of air exchange rate, particle size and injection place on particle concentrations within a reduced-scale room. Building and Environment. 2015;92:246-55.

52. Adeolu M, Alnajar S, Naushad S, Gupta RS. Genome-based phylogeny and taxonomy of the 'Enterobacteriales': proposal for Enterobacterales ord. nov. divided into the families Enterobacteriaceae, Erwiniaceae fam. nov., Pectobacteriaceae fam. nov., Yersiniaceae fam. nov., Hafniaceae fam. nov., Morganellaceae fam. nov., and Budviciaceae fam. nov. International journal of systematic and evolutionary microbiology. 2016;66(12):5575-99.

53. Edwards PR, Ewing WH. Identification of enterobacteriaceae. Identification of Enterobacteriaceae. 1972(Third edition).

54. Seedorf J, Hartung J, Schröder M, Linkert KH, Phillips VR, Holden MR, et al. Concentrations and Emissions of Airborne Endotoxins and Microorganisms in Livestock Buildings in Northern Europe. Journal of Agricultural Engineering Research. 1998;70(1):97-109.

55. Jacobson LD, Bicudo JR, Schmidt DR, Wood-Gay S, Gates RS, Hoff SJ, editors. Air emissions from animal production buildings. Proceedings of the XI International Congress ISAH; 2003.